Sedimentology of the World Class Organic-Rich Lacustrine System, Piceance Basin, Colorado

7

Kati Tänavsuu-Milkeviciene and J. Frederick Sarg

Abstract

The Piceance lake basin formed between *ca* 54–48 Ma years ago, during the early to middle Eocene, and it contains the largest known oil shale resources in the world today (~1.5 trillion bbls in place). Based on the detailed facies and facies association study three small-scale (decimetre to metre) depositional cycles have been separated that characterize deposition along the basin margin and in the deeper part of the basin. Stacked depositional cycles form large-scale depositional sequences (metre to 10's of metres). Depositional sequences characterize significant changes in lake regime and are divided into periods of low, rising, and high lake. During low lake level, main accumulation of deposits occurred in the deeper part of the basin where organically lean deposits formed. Following rising and high lake levels brought thick accumulations of siliciclastic and carbonate deposits along lake margin that were later, during high lake level capped by littoral to sublittoral siltstones and mudstones, and lean oil shales. In the deeper part of the lake thick organically rich deposits formed. The overall lake evolution is characterized by lake stages that reflect long-term changes in the basin controlled by both, climate and tectonics. Lake Stage 1, Fresh to Mesosaline lake was deposited during decreasing tectonic activity and increasing climate control. Lake Stages 2 and 3, Transitional and Highly Fluctuating lake are interpreted to be dominated by an increasingly warm and arid climate and characterized by laterally discontinuous and very rich oil shale deposits. The following Stages 4 and 5, Rising and High lake record the change to a wetter climate and increasing tectonic

K. Tänavsuu-Milkeviciene (✉)
Department of Geology and Geological Engineering,
Colorado School of Mines, Golden, CO 80401, USA

Statoil ASA, Research Centre Rotvoll,
Trondheim NO-7005, Norway
e-mail: KTAN@statoil.com

J.F. Sarg
Department of Geology and Geological Engineering,
Colorado School of Mines,
Golden, CO 80401, USA

M.E. Smith, A.R. Carroll (eds.), *Stratigraphy and Paleolimnology of the Green River Formation, Western USA*, Syntheses in Limnogeology 1, DOI 10.1007/978-94-017-9906-5_7

activity, resulting in increased runoff, development of a widespread deep lake that extended across the Piceance basin, and are marked by the laterally continuous rich oil shale deposits. Stage 6, Closing lake marks high siliciclastic input, the beginning of the closing of the Piceance basin, and progressively decreasing organic richness.

7.1 Introduction

The Piceance basin is one of the three Green River Formation lake basins that formed during the early to middle Eocene and contain a vast amount of oil shale resources. The Piceance basin is estimated to be one of the largest depositories of oil shale in the world known today (~1.5 trillion bbls in place) (Johnson et al. 2010) and is a classic example of a deep organic-rich lake with a mixed carbonate-siliciclastic and evaporite-rich lacustrine depositional system. The Piceance lacustrine basin formed over a period of *ca* 5–6 Myr (Smith et al. 2008, 2010), during which time continuous deposition occurred in the lake. This has led to the formation of thick lacustrine deposits, up to 1,000 m in thickness, in the lake depocenter, in the northern portion of the basin, representing the entire section of the lake evolution.

Because of its high organic content and well-defined organic-rich and organic-poor intervals, rich oil shale zones and lean oil shale zones have been separated in the deeper part of the basin (Cashion and Donnell 1972, 1974). This has also led to the usage of two stratigraphic schemes, one that uses lithofacies, and another that uses these rich and lean zones (e.g., Cole and Daub 1991; Pitman 1996; Dyni 2006; Johnson et al. 2010; Self et al. 2010b). The latter has been important from the industry point of view to identify the organic-rich intervals, whereas the lithologic units give the overview of the lithotypes. Several assessments of the oil shale deposits have been made previously and the distribution of the rich and lean zones within the deeper part of the basin area is well known (Pitman and Johnson 1978; Pitman et al. 1989; Mercier et al. 2009; Johnson et al. 2010). However, rich and lean zones are not well defined along the basin margins and in the southern portion of the basin, and it has been problematic to correlate the basin margin deposits with the deeper basinal deposits (see also Johnson et al. 2010; Johnson 2012).

This paper presents an overview of the main facies and facies associations in the Piceance basin area, describes lateral and vertical variation of facies associations and their depositional relationships. We will also describe sequence stratigraphic units and surfaces, how they form and how they are connected to the formation of the rich and lean oil shale zones. Finally, this work will give an overview of the evolution of the Piceance lake basin and how it responded to the climate and tectonic changes during the early and middle Eocene. Defining the sequence stratigraphic framework, the formation of rich and lean oil shale zones, and the evolution of the Piceance basin could be useful for interpreting other lake basins, especially for understanding the short-term and long-term alternations caused by climate and tectonic changes and how they change throughout lake evolution and for predicting the distribution of facies associations and organic-rich deposits throughout the lake basin.

7.2 Geology and Stratigraphy

During the Laramide Orogeny a series of continental basins, the Piceance basin, the Uinta basin and the Greater Green River basin formed in the Colorado, Utah, and Wyoming, respectively (Dickinson et al. 1988) (Fig. 7.1). Lacustrine deposits formed in mid-latitude warm-temperate to subtropical climate (Sewall and Sloan 2006; Clementz and Sewall 2011). The deposition in lakes was initiated and terminated by tectonic and landscape evolution events convolved with climate effects (Carroll et al. 2006; Davis et al. 2009; Chetel et al. 2011; Tänavsuu-Milkeviciene and Sarg 2012).

For most of their history these non-marine basins were separated from one another by

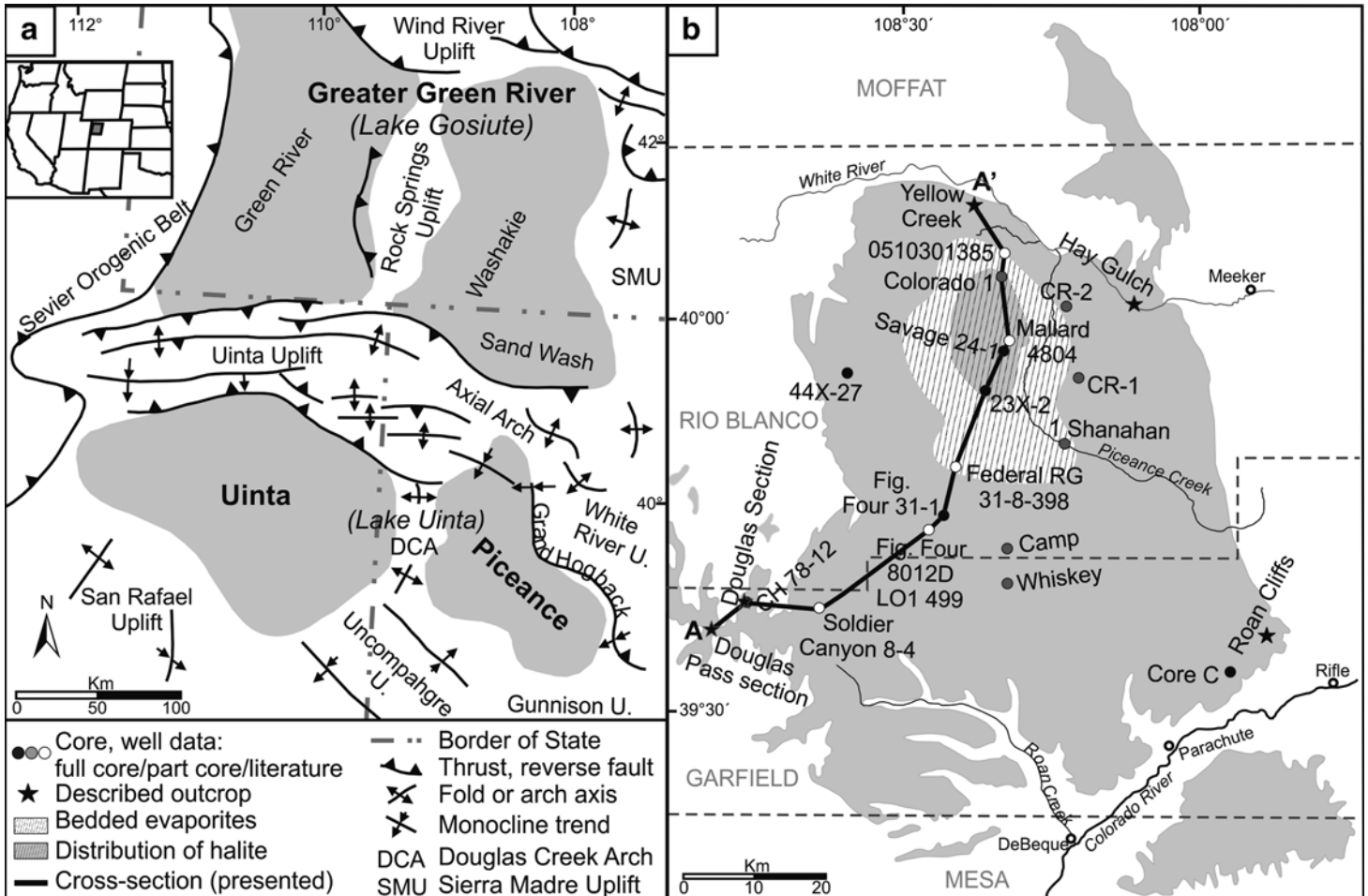

Fig. 7.1 (**a**) Eocene intermountain basins and basin bounding uplifts of the western USA (Modified after Dickinson et al. 1988). The Uinta basin and the Piceance basin form Lake Uinta. (**b**) Close-up map of the Piceance basin with described cores and outcrops from the study area, and the representative cross-section (A-A'). Black circles mark cores, where the entire interval of the Green River Formation was described. *Gray circles* mark cores, where only part of the Green River Formation interval was described. *White circles* mark wells from literature that are used on presented cross-section (A-A'). *Shaded area* in the northern part of the basin indicates distribution of the thick-bedded evaporites, as well as the basin depocenter (After Dyni 1981; Dyni and Hawkins 1981). Cross-section A-A' is shown in Fig. 7.3

anticlinal basement-cored uplifts, and developed as separate lakes, but were at times, connected (Surdam and Stanley 1980; Smith et al. 2008; Davis et al. 2009). The Piceance basin is separated from the Greater Green River basin by the Uinta Mountains to the north and northwest, and from the Uinta basin by the Douglas Creek Arch to the west (Fig. 7.1). When the Piceance basin and Uinta basin were connected they formed a vast lake named Lake Uinta (Fig. 7.1). At times Lake Uinta was connected with the Greater Green River basin (known also as Lake Gosiute) to the north through the Sand Wash basin (Smith et al. 2008; Davis et al. 2009) (see also Fig. 7.1).

The Piceance lake basin covers a portion of northwestern and western Colorado (see Fig. 7.1). Three erosional remnants of previous lake deposits are exposed: the southernmost Grand Mesa *ca* 648 sq km, the middle Battlement Mesa *ca* 285 sq km, and the largest remnant, located north of the Colorado River, and the Piceance Creek covering the northern part of the basin *ca* 4,403 sq km (Young 1995; Johnson 2012, personal communication) and comprising the Roan Plateau. This work focuses on the northern part of the basin. The overall thickness of the Green River Formation varies, and is up to 1,100 m thick in the northern-central part of the Piceance basin.

Deposition of the Green River Formation lacustrine sediments occurred over a period of 5–6 Myr, between *ca* 53 to *ca* 48 Ma (Smith et al. 2008, 2010). The Green River Formation in the study area is subdivided into (1) five members, based on lithology and (2) 17 rich and lean zones, based on kerogen content (Fig. 7.2). The oldest member, the freshwater mollusc-bearing Cow Ridge Member interfingers with the alluvial Wasatch Formation (Fig. 7.2). The base of the Formation is marked by a major transgression of lake deposits and is marked by a distinctive ostracod, oolite, and mollusc-rich bed i.e., Long Point Bed (Fig. 7.2) (Johnson 1984).

The Cow Ridge Member is overlain by mixture of lake-margin fluvial-dominated siliciclastic deposits and microbial and non-microbial carbonates of the Douglas Creek Member in the western and southern parts of the study area. In the eastern and northern parts of the study area marginal wave-dominated siliciclastic deposits with some

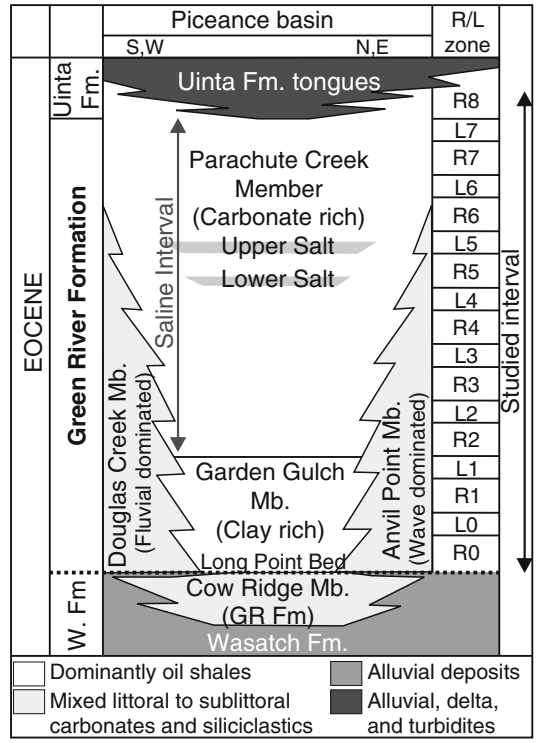

Fig. 7.2 Lithostratigraphic subdivision of the lower and middle Eocene deposits and correlation with kerogen-rich (*R*) and kerogen-poor (*L*) zones in the Piceance basin (Modified after Pitman 1996; Dyni 2006; Johnson et al. 2010; Self et al. 2010b; Rich and lean zones after Cashion and Donnell 1972, 1974). Upper salt and lower salt zones mark the thickest, bedded halite intervals in the basin. The saline interval marks the range of evaporite deposition. Note that the subdivision of the Green River Formation interval into rich and lean zones applies only for the deep, profundal deposits in the basin area

thin microbial carbonate deposits of the Anvil Point Member overlie the Cow Ridge Member (Fig. 7.2). In the central part of the Piceance basin, illitic (clay-rich) oil shale deposits of the Garden Gulch Member overlie the Cow Ridge Member. The thickest and most wide spread part of the Green River Formation, the Parachute Creek Member (Fig. 7.2), consists of calcite and dolomite-rich mudstones. In places, bedded and disseminated evaporites (halite, nahcolite, dawsonite) occur in the Parachute Creek Member (Fig. 7.2). The upper part of the Parachute Creek Member interfingers with the alluvial, deltaic and turbidite deposits of the Uinta Formation (Fig. 7.2). Based on kerogen content, deposits of the Piceance basin are subdivided into nine oil-rich zones (R) and

eight oil-lean zones (L) (Cashion and Donnell 1972, 1974) (Fig. 7.2). The interval of the Green River Formation studied in this work represents the interval between the Long Point Bed and the Uinta Formation sandstones.

7.3 Methods

This study is based on centimeter-scale descriptions of outcrop and core sections, and integrated Fischer assay and gamma ray log data. Data we employed included, (1) six core sections covering the entire Green River Formation interval, (2) six core sections from the Parachute Creek Member, (3) five outcrop sections from the Douglas Creek and Parachute Creek Members, for a total of 13 measured sections, and (4) over 900 Fischer assay and gamma ray well-log data from the Green River Formation (after Mercier et al. 2009; Self et al. 2010a, b) (see Fig. 7.1). This data set allowed interpretation of lateral and vertical facies association relationships, stacking patterns, basin architecture, and changes in depositional processes. Additional published material was used to clarify the depositional environments (Johnson et al. 1988; Johnson 2012).

Integration of facies associations, gamma ray character, and Fischer assay logs were used to correlate main surfaces such as lake stage boundaries, sequence boundaries, transgressive surfaces, and distribution of the sedimentary units in the study area (Fig. 7.3). Tops for rich and lean oil shale zones are after Mercier et al. (2009) and Self et al. (2010a, b) and lake stage intervals are after Tänavsuu-Milkeviciene and Sarg (2012). Described core and outcrop sections were used to identify lateral and vertical variation of facies associations. The cross-section from the southwestern Douglas Creek Arch part of the basin, up to northern part of Piceance basin was chosen to represent the facies associations in whole study area (Figs. 7.1 and 7.3, A-A') because it best displays those relationships. The cross-section is flattened on the Mahogany bed that displays the best laterally continuous oil shale interval, and can be correlated across the entire basin (Fig. 7.3).

7.4 Facies Associations

Deposition in the Piceance basin is characterized by complex depositional system that ranges from alluvial deposits to deep lake deposits (Fig. 7.4).

Twenty-four sedimentary facies (F) were defined by sedimentary structures, textures, and composition (Table 7.1). Sedimentary facies are grouped into 13 facies associations (FA) based on the lateral and vertical association of facies. Facies and facies association descriptions are updated and modified after Tänavsuu-Milkeviciene and Sarg (2012). Facies associations are divided from alluvial to lake deposits. Lake deposits are grouped into lacustrine environments or zones, based on energy level and relative water depth (Fig. 7.4). Lacustrine zones defined by energy levels are: (1) the littoral zone, above fair-weather wave base, (2) the sublittoral zone, between fair-weather wave base and storm wave base, and (3) the profundal zone, below the storm wave base (after Reading and Collinson 1996; Cohen 2003; Renaut and Gierlowski-Kordesch 2010).

7.4.1 Alluvial Facies Association

7.4.1.1 Facies Association 1: Alluvial Deposits

Facies Association 1 (FA1) occurs in the western portion of the basin area, along the Douglas Creek Arch and is characterized by plane-parallel deposits of interbedded mottled (F1), homogeneous (F2), and laminated (F3) mudstones and siltstones, and plane-parallel (F7) or structureless (F10) sandstones (Fig. 7.5a–c: Table 7.1). Mottled, grey to reddish colored mudstones and siltstones (F1) with plant remains and subtle erosional boundaries (Fig. 7.5c) suggest *in situ* early palaeosol development or presence of reworked pedogenic mud aggregates (Wright and Marriott 2007; Müller et al. 2004). Planar-bedded units of plane-parallel (F7) and structureless (F10) siltstones and sandstones interbedded with mudstones indicate sheet-flow deposits (Fig. 7.5a, b), formed as shallow flows spread out across the floodplain (Wakelin-King and Webb 2007). Interbedded siltstones and sandstones are intersected by concave-up, erosionally based

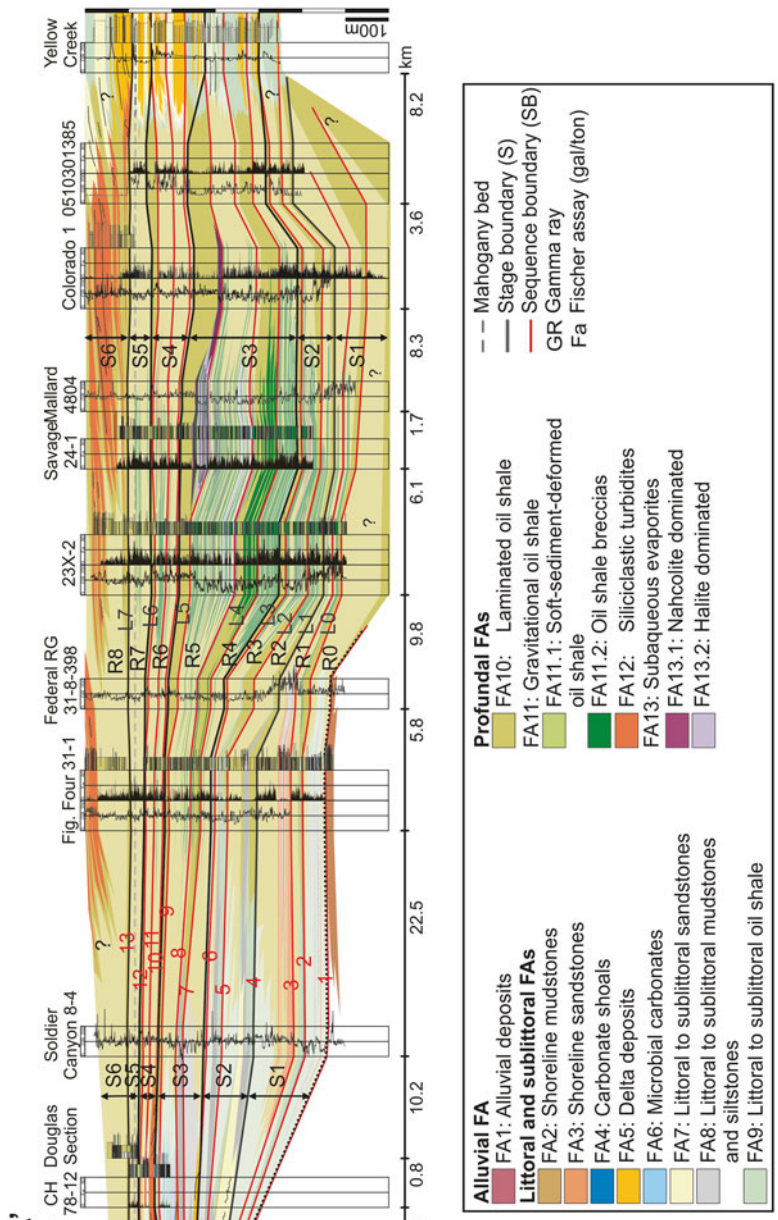

Fig. 7.3 Well-outcrop ross-section of the Green River Formation in the Piceance basin that shows the distribution of the facies associations from the western part of the basin northwards through the deepest part of the basin up to northern margin of the basin (Rich (*R*) and lean (*L*) zones after Cashion and Donnell 1972, 1974; Self et al. 2010b)

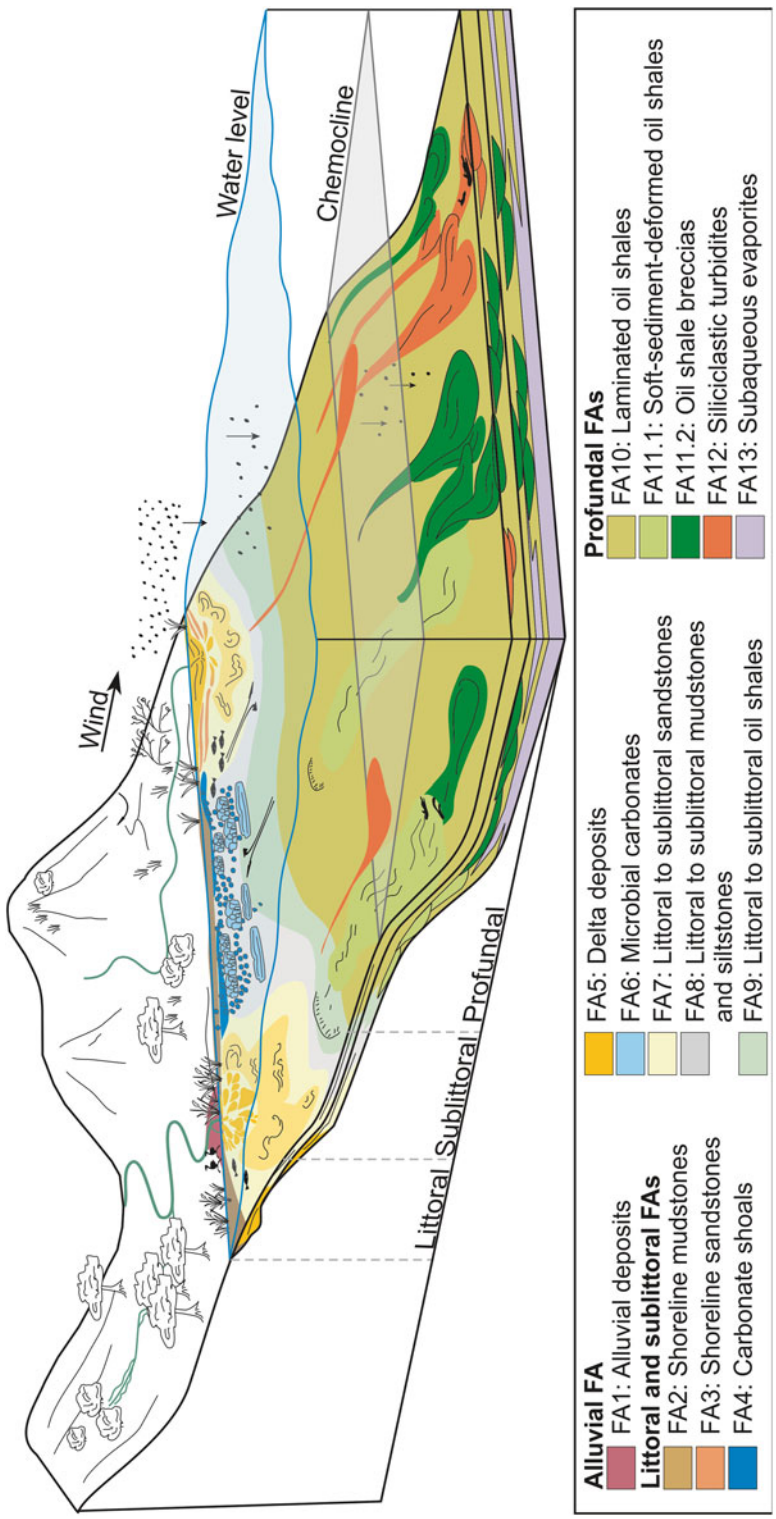

Fig. 7.4 Illustrative depositional model of the Green River Piceance lake basin (Modified after Tänavsuu-Milkeviciene and Sarg 2012) that describes approximate position of facies associations found in the lake basin. Along margin on right is wave-dominated and on left fluvial-dominated deposits. Note, carbonate deposits form at the same time as silicialstic deposits and the occurrence of evaporite deposits within oil shale deposits in the profundal zone

Table 7.1 Facies and their relation to the Facies Associations, Green River Formation, Piceance basin

	Facies	Texture/lithology	Structure	FA
1	Mottled mudstone	Siliciclastic mud and silt	Structureless, red to greenish colored, mottled	1
2	Homogeneous mudstone	Siliciclastic mud and silt	Homogeneous, massive	1, 2, 7, 8
3	Laminated mudstone	Siliciclastic mud, silt, with very fine, fine sand layers	Parallel-laminated	1, 2, 5, 7, 8, 12
4	Wave ripple cross-laminated sandstone	Silt to fine sand	Wave ripple cross-lamination	3, 5.1, 7, 8, 9
5	Current ripple cross-laminated sandstone	Silt to fine sand	Current ripple cross-lamination	5.1, 5.3, 7, 8, 9
6	Climbing ripple cross-laminated sandstone	Silt to fine sand	Climbing ripple cross-lamination	5
7	Plane-parallel sandstone	Silt to medium sand	Sub-horizontal lamination	5.1, 5.2, 7, 12
8	Cross-stratified sandstone	Silt to medium sand	Planar and trough cross-stratification	3, 5
9	Hummocky, swaley cross-stratified sandstone	Silt to fine sand	Low angle, hummocky, swaley cross-stratification	3
10	Structureless sandstone	Fine sand to gravel	Structureless, amalgamated, normally graded, ungraded. Occur rip-up clasts	3, 5.1, 5.3, 12
11	Conglomerate	Granule to pebble	Massive, intraformational rip-up clast conglomerate	3, 5.1, 5.3
12	Microbial carbonates	Lime mudstone to grain-rich bindstone	Finely-laminated, domal stromatolites, thrombolites, shrub-like features, intraclasts	2, 6
13	Nonskeletal limestone	Calcitic mixed packstone to grainstone	Oolites, pisolites, carbonate intraclasts, minor bioclasts; massive, plane-parallel, cross-stratified	4, 6
14	Molluscan limestone	Calcitic coquina	Gastropods, bivalves, structureless or plane-parallel	4
15	Intraclastic mudstone	Carbonate mudstone clasts in a siliciclastic mud matrix		2
16	Finely-laminated oil shale	Dominantly dolomitic kerogen-rich mudstone	Parallel-laminated	10
17	Illitic oil shale	Kerogen-rich mudstone, clay-rich	Parallel-laminated, in places also ostracod-rich	9, 10
18	Laminated silt-rich oil shale	Kerogen-rich mudstone, dominantly carbonate-rich, with silt to very fine sand	Parallel-laminated, minor silt to sand layers and lenses	9
19	Wavy-laminated oil shale	Kerogen-rich mudstone, clay-rich or carbonate-rich	Wavy to disrupted lamination	9, 10, 11.1
20	Soft-sediment-disturbed oil shale	Dominantly dolomitic kerogen-rich carbonate	Overturned lamina, microfaulted, incipient brecciation	11.1
21	Oil shale breccia	Matrix-supported breccias, dominantly dolomitic kerogen-rich mudstone with clasts (clasts mm to cm in scale)	Organic, carbonate, and siliciclastic clasts. In places, nahcolite clast. Carbonate clasts are homogeneous or finely laminated. Occur graded bedding	11.2

(continued)

Table 7.1 (continued)

	Facies	Texture/lithology	Structure	FA
22	Nahcolite		Nodules and/or crystals to crystal accumulations form mm-dm thick beds	10, 11.2, 13
23	Halite		Hopper crystals and bottom growth crystals form mm-cm thick beds	13
24	Dawsonite		Fine crystals	13

Updated and modified after Tänavsuu-Milkeviciene and Sarg (2012)

decimeter to meters thick and several meter wide sandstone units that continue as thin, decimeters thick single very fine to fine-grained sandstone beds (Fig. 7.5a). These erosionally based sandstones are described as flood channel and levee deposits (Müller et al. 2004; Wakelin-King and Webb 2007). Additionally, decimeter thick, up to several meters wide siltstone to very fine-grained sandstone bodies with erosional lower bounding surfaces that contain coarser grained sandstone lenses and beds are observed in places, and load into underlying finer-grained deposits. These suggest separate flood channels (Fig. 7.5a–c). Overall, the dominance of planar beds, scours and mud layers, as well as the occurrence of possibly reworked pedogenic deposits and the association FA1 with deltaic deposits (FA5) and microbial carbonates (FA6) suggest deposits formed in a dryland river system, in floodplain or as overbank deposits in the vicinity of the lake (Wakelin-King and Webb 2007; Wright and Marriott 2007).

7.4.2 Littoral and Sublittoral Facies Associations

7.4.2.1 Facies Association 2: Shoreline Mudstones

Facies Association 2 (FA2) occurs within the lake margin (Fig. 7.4) and in places, can be traced laterally hundreds of meters along the outcrop (Fig. 7.5e). FA2 consists of homogeneous (F2) or laminated (F3) mudstone and siltstones in association with microbial carbonate (F12) and intraclastic mudstone (F15) (Table 7.1).

7.4.2.2 Facies Association 3: Shoreline Sandstones

Facies Association 3 (FA3) occurs at the margins of the lake, dominantly in the eastern and northern parts of the basin, in association with delta (FA5) deposits and littoral to sublittoral sandstones (FA7) (Figs. 7.3, 7.4 and 7.6, Section 1). This FA consists of gradationally based or sharp based fine-grained to medium-grained quartz sandstones with wave rippled cross-lamination (F4), climbing ripple cross-lamination (F6), low-angle cross-stratification (F8), and hummocky and swaley cross-bedding (F9), or sharp based fine-grained to coarse-grained amalgamated, normally graded or ungraded (F10) sandstones and sub-horizontal or parallel-laminated gravel beds (F11) (Fig. 7.6a and Section 1; Table 7.1). Medium to coarse-grained sandstones with gravel beds, occurrence of graded bedding, amalgamation, and hummocky and swaley cross-stratification suggests storm wave activity and deposition in the lake shore area (Renaut and Owen 1991; Bray and Carter 1992; Ilgara and Nemec 2005). These deposits are interpreted to have formed due to longshore transport in a shoreline setting (Fig. 7.4). Alternatively, they could have been formed as wave reworked deposits in wave-dominated delta deposits (see Fig. 7.6, Section 1). However, deposits brought in by river discharge and reworked into shoreface deposits makes the distinction between delta and shore deposits difficult (see also Bhattacharya and Giosan 2003; Smith et al. 2005) (see Figs. 7.4 and 7.6, Section 1).

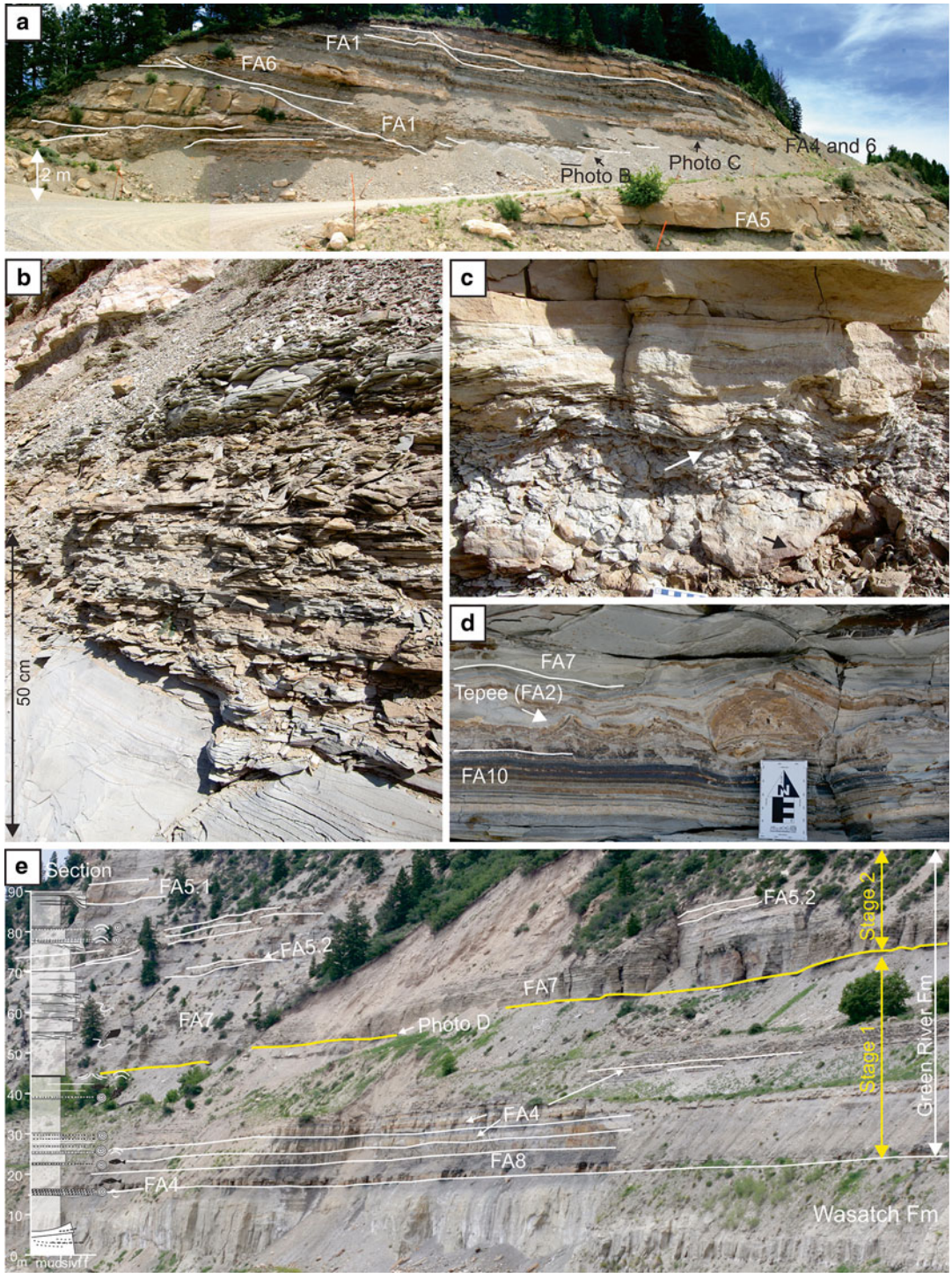
a
FA1
FA6
FA1
2 m
Photo B
Photo C
FA4 and 6
FA5
b
50 cm
c
d
FA7
Tepee (FA2)
FA10
e
Section
FA5.1
FA5.2
FA7
Photo D
FA4
FA8
FA4
FA5.2
FA7
Stage 2
Stage 1
Green River Fm
Wasatch Fm
m mudstone

7.4.2.3 Facies Association 4: Carbonate Shoals

Facies Association 4 (FA4) occurs in the marginal areas, dominantly in the western and southern parts of the basin, is laterally equivalent to shoreline sandstones (FA3), and occurs in association with microbial carbonates (FA6), littoral and sublittoral mudstones (FA8), and littoral to sublittoral oil shales (FA9) (Figs. 7.3, 7.4, 7.5e, and 7.6b). This FA is composed of sharply based, massive or plane-parallel, non-skeletal coated carbonate grainstones and packstones (F13), and coquina (F14) beds of moderately to very well sorted oolites, with ostracode or quartz grain cores, pisoids and peloids, and siliciclastic to microbial carbonate rip-up intraclasts (Figs. 7.5e and 7.6b; Table 7.1) (Sarg et al. 2013). This indicates the deposition in high-energy carbonate shoals parallel to the lakeshore (Milroy and Wright 2002; McGlue et al. 2010). Alternately, deposits of FA4 could indicate shallow littoral deposits (Milroy and Wright 2002), or they could have been redistributed by wind activity and shoreline currents into deeper, lower energy sublittoral environments (Milroy and Wright 2002; McGlue et al. 2010) (see Fig. 7.4). In places, carbonate grainstones display reverse grading where the coarser grained oolites or pisolites occur in the upper portion of the bed, suggesting episodic reworking in variable energy environment.

7.4.2.4 Facies Association 5: Delta Deposits

Facies Association 5 (FA5) occurs across the basin margins and it consists of depositional packages, where sandstone and mudstone deposits are separated by littoral to sublittoral mudstone to sandstone deposits of FA7 and 8 (Figs. 7.3, 7.4, and 7.6c, d). In a few places, mudstones from FA2 separate sandstone units. Three types of depositional packages are classified here. Type 1 (FA5.1) is formed from laterally continuous sandstone bodies that are separated by laminated mudstone and siltstone (F3) beds, a few centimeters to tens of centimetrers thick. No desiccation cracks or root structures have been found in these interfingered mudstone or siltstone deposits. Two types of depositional units occur within Type 1 sandstone package. The first type of depositional unit is characterized dominantly by sharp-based very fine-grained to fine-grained sandstones that coarsen upward or have no particular grain-size trend and consists of climbing ripple cross-lamination (F6), plane parallel (F7), and low angle cross-stratification (F8) (Fig. 7.6c). Locally, current ripple cross-lamination (F5), structureless (F10), or wave-modified deposits occur. Intraformational clasts (F11) of mudstone or siltstone, plant remains and fish remains occur on the erosional lower bounding surfaces (Fig. 7.6e, f). The second type of depositional unit is characterized by gradationally based upward-coarsening deposits that are composed of wave ripple cross-laminated (F4) and low angle cross-stratified (F8), very fine-grained to fine-grained sandstone deposits (Fig. 7.6d) and are associated with coarser-grained sandstones of shoreline mudstones (FA3).

These laterally extensive depositional units are interpreted as mouth bar deposits, where dominantly sharp-based deposits that consist of climbing ripple and plane-parallel sandstones are interpreted as river-dominated delta-front deposits (Fig. 7.6c). Gradationally based

Fig. 7.5 Representative photographs of the lake margin deposits. (**a**) Highly fluctuating cycles of marginal lake deposits that display close relationship between alluvial plane-bedded dry river deposits (*FA1*) and are interbedded with carbonate shoal (*FA4*), microbial carbonates (*FA6*), and delta deposits (*FA5*). (**b**) Planar-bedded overbank or floodplain deposits with silty and sandy sheet flow deposits (*FA1*). (**c**) Mottled, inclined mudstone with organic rip ups (*black arrow*), formed as plaeosol or as reworked pedogenic mud aggregates (*FA1*) overlain by sandstones with load structures (*white arrow*). (**d**) Tepee structures (FA2) followed by microbial carbonates (*FA6*), the base of the tepee structures marks SB4, and boundary between Stage 1 and 2. The stratigraphic position of the bed is shown on Fig. 7.5e. (**e**) Mixed siliciclastic and carbonate facies associations formed in the western part of the basin that characterize deposits formed in the lower Green River Formation, Stage 1 and 2. Note the alternation between carbonate shoal (FA4) and sublittoral to profundal oil shale (*FA9* and *FA10*) deposits in Stage 1, and the high siliciclastic input in the beginning of Stage 2

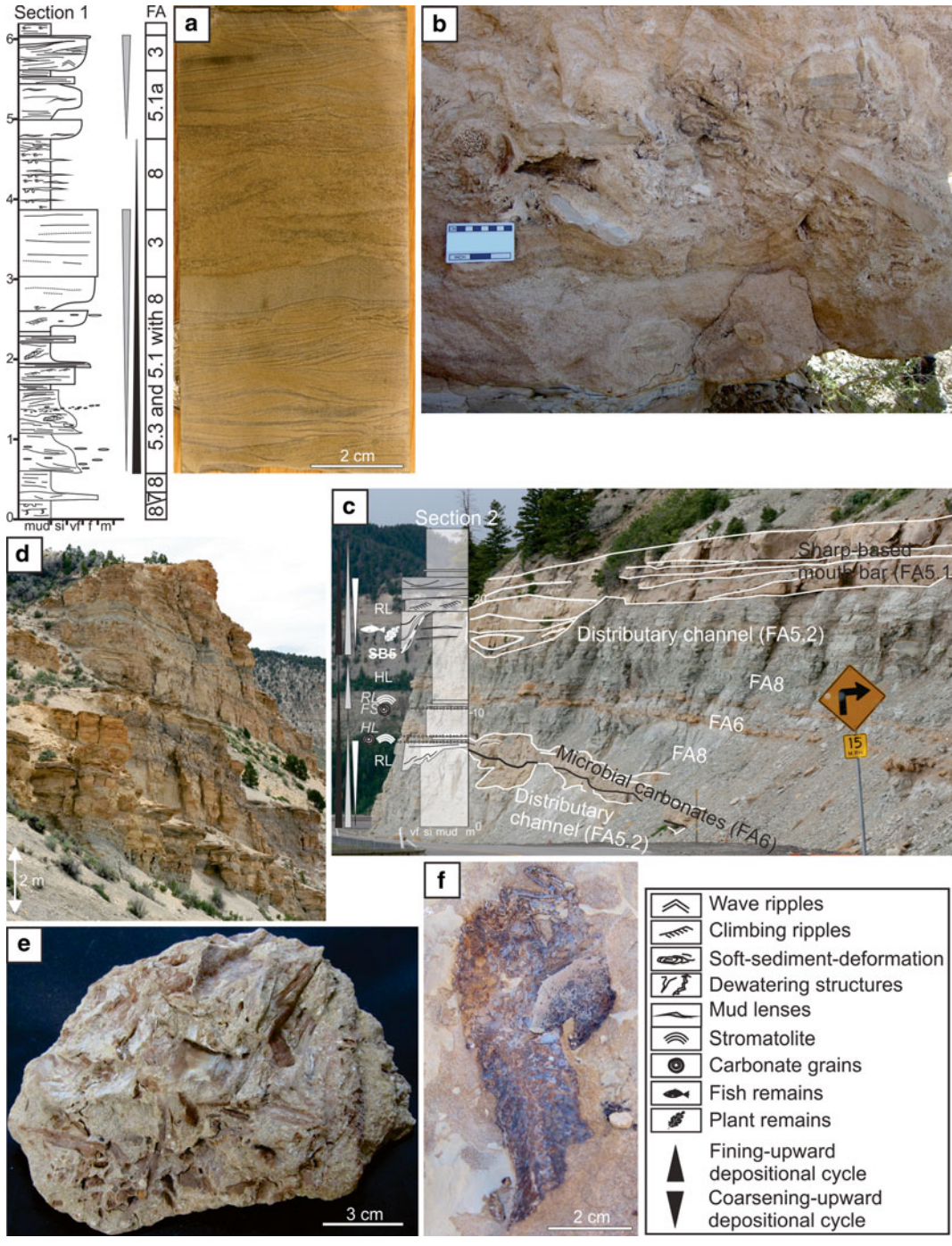

Fig. 7.6 Representative photographs of the lake margin deposits. Section 1 marks wave-dominated deposits and relationship between FA3 and FA5. (**a**) Bundled upbuilding wave ripple cross-laminated shoreline deposits (FA3). (**b**) Storm-generated intraclastic carbonate shoal (FA4) with rip-up microbial carbonates, oncolites, oolites, and siliciclastic mudstone clasts. (**c**) Lake margin deposits that form upward-fining depositional cycles from distributary channels (5.2) and bars (5.1) upwards into microbial carbonates (FA6) that are covered by littoral to sublittoral siltstones (FA8). (**d**) Wave-dominated delta (FA5) to shoreline (FA3) deposits. (**e**) Organic rip-up clasts, wood pieces on the lower bounding surface of the mouth bar. (**f**) Fish fossil found on the lower portion of the mouth bar deposits

deposits, with wave-dominated structures in association with FA3 are interpreted as wave-dominated delta-front deposits (Renaut and Tiercelin 1994; Buatois and Mangano 1995; Schomacker et al. 2010) (Figs. 7.3, 7.4, and 7.6d). Likewise, some wave ripple dominated deposits could indicate wave-reworked shoreline sandstones formed in the wave-dominated delta setting (see also FA3 and Fig. 7.4) (Bhattacharya and Giosan 2003; Smith et al. 2005).

The second type of depositional package, Type 2 (FA5.2), is composed of laterally discontinuous sandstones of low angle and trough cross-stratified (F8), plane-parallel (F7) and climbing ripple (F6) cross-laminated deposits with concave-up basal scour and near horizontal upper surfaces. In places, heterolithic successions of parallel-laminated (F3) mudstones and siltstones and interbedded sandstones fill the scours (Fig. 7.6c; Table 7.1). Locally, the basal surface is undulating and contains large-scale soft-sediment deformation, comprised of small-scale (centimeters in size) and large-scale (decimeters and meters in size) slump and load structures (Fig. 7.6c). These erosionally based structures with no subaerial features suggesting channel deposits that formed in a delta front area as distributary channels to mouth bars (Olariu and Bhattacharya 2006; Schomacker et al. 2010). Sandstone-dominated channel fills are interpreted to have formed in the proximal delta front area. Heterogeneous channels fills, as well as channels with undulating scour boundaries, and load deposits are interpreted to have accumulated in a more distal position of the delta front.

Type 3 depositional packages in this facies association (FA5.3) are composed of very fine to fine-grained cross-stratified (F8) and climbing (F6) to current (F5) ripple cross-laminated sandstones, or medium to coarse-grained structureless sandstones (F10) that pass upwards into parallel-laminated (F3) mudstones and siltstones (Fig. 7.6, Section 1; Table 7.1). The sandstone to mudstone stacked depositional units in Type 3 (FA5.3) are interpreted as turbidites formed dominantly during hyperpycnal density flows in the distal part of the delta front (see also Renaut and Tiercelin 1994) (Fig. 7.4). This is also supported by the aggradational pattern of depositional packages and the vertical relationship with Type 1 (FA5.1) mouth bar deposits (Fig. 7.6, Section 1).

7.4.2.5 Facies Association 6: Microbial Carbonates

Facies Association 6 (FA6) consists of millimeter to centimeter-scale, thinly laminated limestones interbedded with boundstones displaying small vertically oriented shrub-like features, and massive limestones displaying clotted fabric (Fig. 7.7a) that are interpreted as microbial carbonate deposits: stromatolites and thrombolites formed in the marginal areas of the lake (Rainey and Jones 2009; Gierlowski-Kordesch 2010; Wright 2012) (see Figs. 7.3 and 7.4). Laminated carbonates (F12) occur as laterally continuous, millimeter to centimeter-thick horizontal carbonate layers, and as beds and laterally linked or discontinuous columns, tens of centimeters to 1 m thick, with well-developed domal heads (Fig. 7.7a, b). Different desiccation features such as mudcracks or large-scale sheet cracks have not been observed. The lack of desiccation features suggests that these carbonates formed dominantly in a subaqueous setting in the lake, in the littoral and sublittoral zones (see also Cohen et al. 1997). Intraclastic carbonate and nonskeletal lime packstones/grainstones (F13) containing oolites and pisolites occur as thin layers or beds and in pockets between microbialite mounds.

These mixed microbialite and nonskeletal deposits probably formed in the shallower, higher energy littoral zone to upper sublittoral zone, whereas laterally continuous laminated deposits with less distinctly developed domal heads are interpreted to have been deposited in the deeper, sublittoral zone (Platt and Wright 1991; Cohen et al. 1997; Renaut and Gierlowski-Kordesch 2010; Sarg et al. 2013) (see Fig. 7.7a, b). Thin, millimetre-thick laminated carbonates in association with sublittoral to profundal oil shales, FA9 and 10 (see Fig. 7.7b) are interpreted to be microbialites formed in the deepest, sublittoral zone.

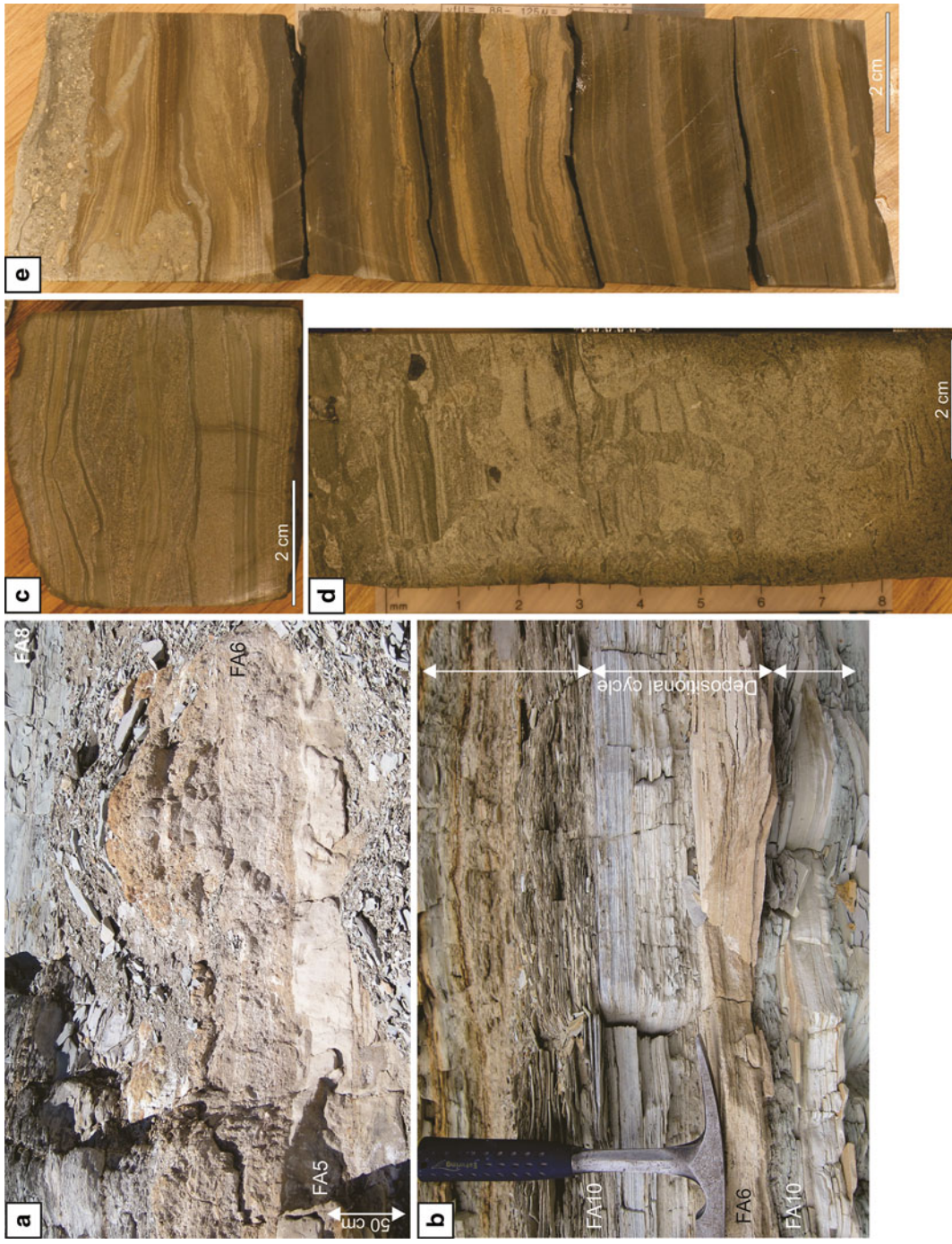

Fig. 7.7 Representative photographs of the littoral to sublittoral lake deposits. (**a**) Microbial carbonates (FA6) that lay sharply on delta sandstones (FA5). Lower portion of the carbonate unit consist of brecciated carbonate beds that are stabilized by stromatolites and continue upwards into thrombolites. Microbial carbonates are overlain by littoral to sublittoral siltstones (FA8). (**b**) Deeper microbial carbonates (FA6) formed in the lower sublittoral or in the most upper portion of profundal part of lake, interbedded with profundal, organic-rich, laminated oil shale (FA10) deposits. (**c**) Mud draped thin sand layers and bidirectional wave ripples in the littoral and sublittoral sandstones (FA7). (**d**) Possible burrows in the littoral to sublittoral sandstones (FA7). (**e**) Sublittoral oil shale (FA9) with thin siltstone and sandstone layers

7.4.2.6 Facies Association 7: Littoral to Sublittoral Sandstones

Facies Association 7 (FA7) consists of very fine- to fine-grained plane-parallel (F7), thinly bedded sandstones. In places, wave ripple cross-lamination (F4), wave-modified deposits, or less commonly, current ripple cross-lamination (F5) occur (Fig. 7.7c; Table 7.1). This facies association is interpreted to have been deposited basinward from delta (FA5) sandstones and forms in places in the prodelta part of the deltaic deposits (FA5) (see Figs. 7.3, 7.4 and 7.5e, Section). However, FA7 also occurs basinward from shoreline sandstones (FA3) (Figs. 7.3 and 7.4), and is therefore recognized as a separate facies association and is interpreted to have formed in the distal part of areas subject to higher siliciclastic input, filling interdistributary areas. Soft-sediment-deformation features, such as small-scale (centimeter-thick) load casts, slumps, ball and pillow structures, and large-scale (meter-thick) slump structures are abundant. Abundant soft-sediment deformations indicate post-depositional processes like rapid deposition or loading by landslides or waves (Sabato 2007; Bridge and Demicco 2008). Vertical to sub-vertical, lenticular, deformed cracks, a few millimeters to centimeters in length and filled with sand size deposits occur in mudstones and siltstones below the sandstones. These features are connected with the overlying sand and in places show lateral and vertical linkage with other sand intervals, and are therefore interpreted as interstratal dewatering structures, formed due to the compaction of mudstones layers during burial (Tanner 1998). In places, cm-scale vertical features cross-cut deposits that suggest bioturbation (Fig. 7.7d).

7.4.2.7 Facies Association 8: Littoral to Sublittoral Mudstones to Siltstones

Facies Association 8 (FA8) consists of interfingering parallel-laminated (F3) or massive (F2) mudstones to siltstones with up to fine-grained wave ripple cross-laminated (F4) or less commonly, current ripple cross-laminated (F5) sandstone lenses, lamina, and beds several centimeters thick (Figs. 7.6c and 7.7a, e; Table 7.1). Interfingering of mudstones with ripple cross-laminated sandstones indicates deposition above storm wave base. These dominantly fine-grained sediments are interpreted to be deposited in the areas with limited siliciclastic input (Figs. 7.3 and 7.4), in lower littoral to sublittoral zones (Smith et al. 2005; Keighley 2008). Small-scale soft-sediment deformation features (centimeter-thick), such as load casts, slumps, ball and pillow structures occur in these deposits and indicate post-depositional processes suggesting rapid deposition or loading by landslides or waves (Sabato 2007; Bridge and Demicco 2008). Horizontally oriented triangular features that resemble cracks, a few millimeters to centimeters in length, and filled with sand size deposits occur in mudstones and siltstones. These features are interpreted here as syneresis cracks as they are not connected vertically with any other bed or layer and have been interpreted to be formed due to the swelling or shrinking of clays caused by the salinity changes (Plummer and Gostin 1981).

7.4.2.8 Facies Association 9: Littoral to Sublittoral Oil Shale

Facies Association 9 (FA9) consists dominantly of laminated silt-rich oil shale (F18) and undulating, wavy-structured oil shale (F19) deposits that indicate a low-energy environment (Table 7.1). In the lower part of the Green River Formation these deposits are illite-rich (F17). Oil shale deposits interfinger with thin, millimeter to centimeter-thick, structureless, normally graded or wave ripple cross-laminated (F4) and current ripple cross-laminated (F5) very fine- to fine-grained sandstone layers and lenses (Fig. 7.7e). An association of mudstones with siltstones and sandstones suggest deposition in the nearshore lower littoral to sublittoral zones, above storm wave base (Renaut and Tiercelin 1994; Smith et al. 2005), in the distal portions of carbonate shoals (FA4), microbial carbonates (FA6), and littoral to sublittoral mudstones (FA8) (Figs. 7.3 and 7.4).

7.4.3 Profundal Facies Associations

7.4.3.1 Facies Association 10: Laminated Oil Shale

Facies Association 10 (FA10) occurs as laterally relatively continuous units across the lake basin

and is composed of rhythmically millimeter laminated, light brown to dark brown, black or gray kerogen-rich (dark) and kerogen-poor (light) mudstone i.e., oil shale couplets (F16) (Fig. 7.8a). The top and the base of each lamina are generally distinct and sharp. In the lower part of the Green River Formation, oil shale is illite-rich (F17) and in the middle and upper part of the formation it is carbonate-rich (F16). Dominantly mud-sized deposits suggest deposition below the storm wave base in a profundal environment. The dark to light lamina may be related to short-term variation in sediment supply, periodic algal blooms, or individual floods (Renaut and Gierlowski-Kordesch 2010; Ghadeer and Macquaker 2012). Undulating, wavy, disrupted oil shale (F19) and in places, millimeter-thick siltstone to very fine-grained sandstone lamina and lenses occur in deposits suggesting deposition due to current and mass flows caused by storms or sediment gravity flows (Schieber 2011; Ghadeer and Macquaker 2012) (Fig. 7.8a). In places, bedding is sharply constricted giving a morphology resembling loops or links of a chain, i.e., loop bedding (Fig. 7.8a). Nahcolite crystals and nodules (F22) of variable size, from a few centimeters to tens of centimetrers in diameter, occur within this facies association (Fig. 7.8b). Pyrite occurs as small crystals within the deposits or as rinds around the nahcolite nodules. No trace fossils were found. Relatively continuous units, finely laminated with some disturbed sedimentary features, occurrence of pyrite, and lack of trace fossils indicate deposition in meromictic conditions in a deep-lake environment (Demaison and Moore 1980; Kelts 1988; Johnson and Graham 2004; Scholz et al. 2011) (Figs. 7.3 and 7.4).

7.4.3.2 Facies Association 11: Gravitational Oil Shale

Facies Association 11 (FA11) occurs as laterally discontinuous units of contorted, soft-sediment-deformed, kerogen-rich or kerogen-poor deposits in which the original texture and stratification have been obliterated (Fig. 7.8c–f). Deposits of FA11 occur as stacked packages or single beds from centimeter to several meters in thickness in association with laminated oil shales (FA10), siliciclastic turbidites (FA12), and subaqueous evaporites (FA13) (Figs. 7.3 and 7.4). The thickness and frequency of FA11 decrease towards the lake margins (Fig. 7.3, compare 23X-2 and Fig. Four 31-1). No desiccation cracks, bioturbation, ripple cross-lamination or algal structures have been observed from these deposits. Deposits of FA11 are divided into two types, based on texture and structure. Type 1 (FA11.1) is composed of soft-sediment folds, overturned strata (F20), and disrupted (F19) deposits (Fig. 7.8d; Table 7.1) that formed as slide and slump deposits that were transported for a short distance. The scale of deformed deposits varies greatly from millimeters to metres.

Type 2 (FA11.2) consists of blebby appearing and matrix-supported oil shale deposits containing angular, sub-angular, and sub-rounded clasts ripped up from the surrounding environment (F21), including carbonate clast, siliciclastic clasts, organic rip-ups and evaporite clasts (Fig. 7.8c, f; Table 7.1). The amount and occurrence of clasts in these deposits is variable and they form normally graded beds or are randomly distributed. The upper and lower bounding surfaces can be sharp, erosional or gradational. In places, nahcolite nodules (F22) have formed in deposits. Thick units of FA11.2 are interpreted as amalgamated slump and debris-flow deposits formed due to higher energy turbulent currents (Shanmugam 2000; Arnott 2010) (Figs. 7.3 and 7.4).

The occurrence of contorted, soft-sediment-deformed, and blebby deposits in association with finely laminated deposits of FA10, and the lack of shallow water indicators suggests that deposits of FA11 formed as gravitational deposits in the profundal areas (see also Dyni and Hawkins 1981; Gierlowski-Kordesch and Rust 1994; Keighley 2008) (Figs. 7.3 and 7.4).

7.4.3.3 Facies Association 12: Siliciclastic Turbidites

Facies Association 12 (FA12) consists dominantly of well to very well sorted siltstones to sandstones that form sharp-based centimeter to a few meters thick normally graded or ungraded depositional cycles separated by laminated and

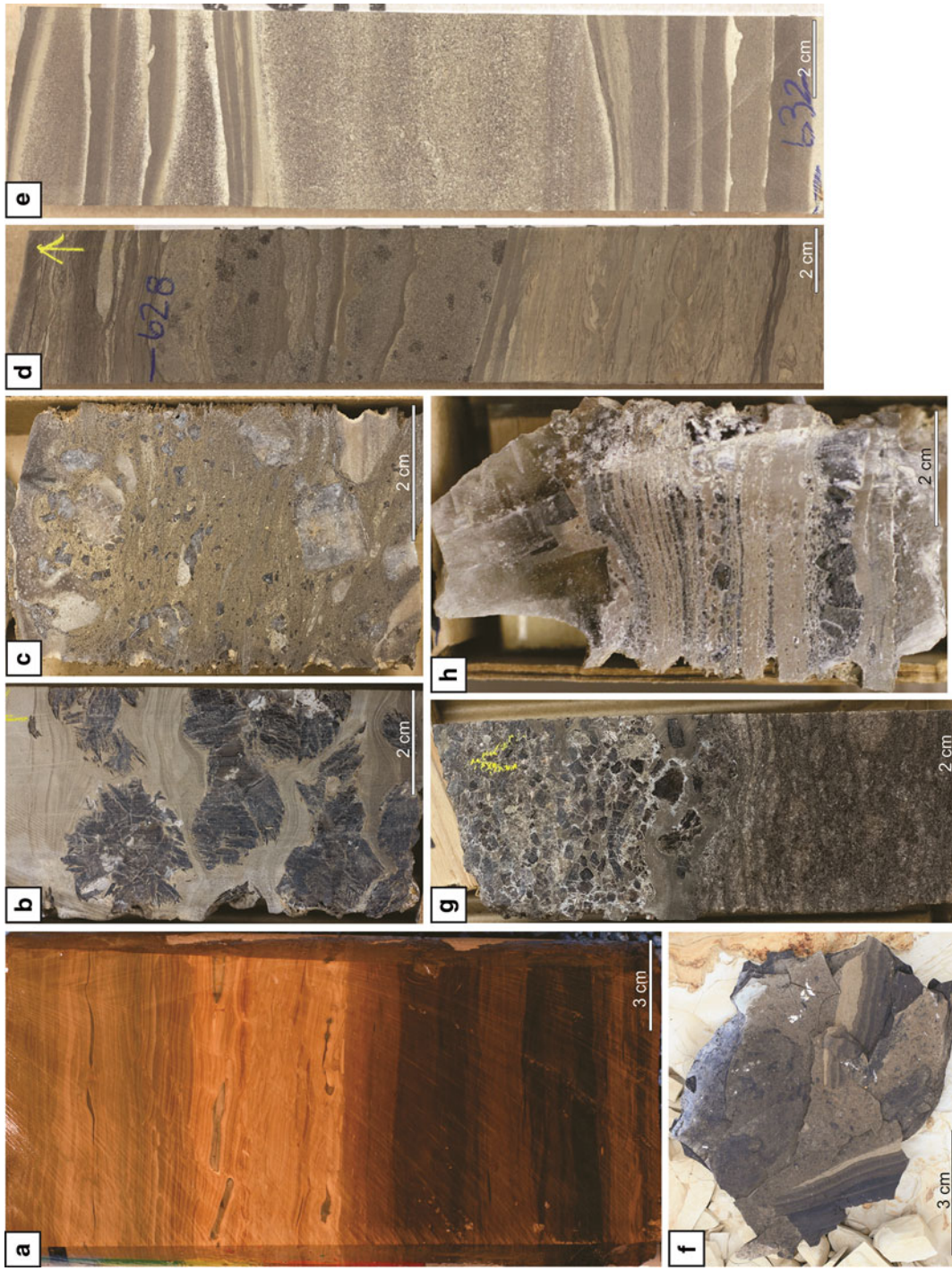

Fig. 7.8 Representative photographs of the profundal lake deposits. (**a**) Disrupted oil shale (FA10). Sharp difference in color marks the difference in organic-richness of deposits, the lower darker portion is richer and the upper portion of the core interval is leaner. (**b**) Laminated oil shale (FA10) with nahcolite nodules. Note the deformation features greater by the nodule growth. (**c**) Oil shale breccia (FA11.2) with evaporite rip-ups. (**d**) Soft-sediment-deformed oil shale (FA11.1) overlied by siliciclastic turbidites (**e**) Upward-fining medium-grained sandstone to mudstone siliciclastic turbidite (FA12) units. (**f**) Bedding-plane view of oil shale breccia (FA11.2), with organic clasts. (**g**) Nahcolite mush and crystal growth (FA13.1). (**h**) Halite bottom growth (FA13.2) and halite to nahcolite laminites (FA13)

soft-sediment deformed mudstones of FA10 and FA11.1, respectively (Fig. 7.8d, e). Load and flame structures occur on bedding planes that suggest rapid depositional rates (Fig. 7.8d). Normally graded depositional units start with coarse to fine-grained structureless (F10) sandstones and grade upwards into parallel-laminated fine to very fine-grained sandstones (F7) or parallel-laminated siltstones (F3) (Fig. 7.8e). Angular to subangular rip-up clasts, as oil shale rip-ups and plant fragments are common, and occur distributed within the sandstone bed or follow bedding planes (Fig. 7.8d). Deposits form stacked packages where the thickness of sandstone to siltstone units decreases upwards and continue into fine-grained sandstones with oil shale rip-ups (Fig. 7.8d). In places, vertical, deformed features, filled with sandstones and connected with overlying sandstones, i.e., water escape structures, occur in the underlying facies associations. These sedimentary structures indicate sediment-gravity flows, principally turbidity currents probably triggered by high intensity storms or river floods (Buatois and Mangano 1995; Johnson and Graham 2004; Osleger et al. 2009) (Figs. 7.3 and 7.4), where upward-fining depositional units are interpreted to indicate Bouma division (after Bouma 1962): structureless, normally graded or ungraded sandstones equate to the Ta, planar-laminated sandstones to the Tb, and planar-laminated siltstones to the Td division (Fig. 7.8e). The association of FA12 with FA10 and FA11.1 suggest deposition in the deep-water, profundal area (see Figs. 7.3 and 7.4).

7.4.3.4 Facies Association 13: Subaqueous Evaporites

Facies Association 13 (FA13) is composed of a few to tens of centimeters thick beds and scattered crystals of nahcolite (F22), halite (F23), and dawsonite (F24) (Fig. 7.8g, h) that occur in association with laminated and gravitational oil shales of FA10 and 11 (Figs. 7.3 and 7.4; Table 7.1). No dissolution surfaces have been found within these deposits. Because dawsonite occurs only as minute crystals, disseminated throughout the oil shale and can be digenetic in origin (Boak and Sheven 2015), it's visual detection usually is difficult or impossible, it is not described future in this work (for additional information see Smith and Milton 1966; Brownfield et al. 2010). Deposits of this facies association are divided into two types. Type 1 (FA13.1) consists dominantly of nahcolite (F22) that occurs as tan to light brown closely to loosely packed crystal accumulations and dark-brown to black fine-grained nodules and radiating nodular aggregates, occasionally rimmed with pyrite (Fig. 7.8b, g, h). Nahcolite crystal accumulations form in many places, upward-fining beds, where the frequency and amount of crystals decrease upwards, and in the upper part, deposits transition gradually into laminated oil shales (FA10). Nahcolite nodules are a few to tens of centimeters in diameter, and appear scattered throughout the deposits or in parallel-bedded zones in association with FA10 and FA11 (Fig. 7.8b). In places, they are rimmed with pyrite. Type 2, (FA13.2) halite (F23) is present as clear to gray crystal cubes, hopper crystals, intra-sediment crystals, and bottom growths within nahcolite deposits and carbonate muds (Fig. 7.8h). Commonly, halite forms couplets with nahcolite, with thicknesses that range from a few millimeters to centimeters (Fig. 7.8h).

FA13 is interpreted to have formed in water saturated with bicarbonate, and periodically with sodium chloride. Laminated, coupled deposits suggest cyclic and perhaps seasonal precipitation. Because depositional rates can be very rapid, there is no evident correlation between crystal size and water depth (Cohen 2003). The occurrence of halite and nahcolite crystals, beds, couplets, bottom growths, and the lack of dissolution features in evaporites and desiccation features in over and underlying deposits of FA10 and FA11, suggest evaporite growth in a standing body of water, in a meromictic lake (Hardie et al. 1978; Last and Vance 1997; Schubel and Lowenstein 1997; LaClair and Lowenstein 2009) (see Fig. 7.3).

7.5 Stratigraphic Architecture

7.5.1 Basin Evolution and Lake Stages

The Green River paleo-lake underwent a long-term evolution that can be described in a series of lake stage units that are tens to hundreds of meters thick (Tänavsuu-Milkeviciene and Sarg 2012). This long-term evolution over a period of about 6 My occurred in response to tectonic and climate changes during early to middle Eocene time. Lake stage depositional packages that characterize lake evolution reflect variation in facies association distribution, richness of oil shale, water chemistry, degrees of lake restriction and salinity, and siliciclastic sediment input (Tänavsuu-Milkeviciene and Sarg 2012) (Table 7.2). Six lake stages have been separated, based on large-scale changes in sedimentological patterns and depositional trends (Table 7.2). Stages do not follow lithological units, i.e., members of the Green River Formation. Broadly, lake stages characterize genetically related units that occur at a particular period during the lake evolution. Lake stages are composed of groups of sequences, but they do not form larger sequences or sequence sets (Figs. 7.3 and 7.10). Boundaries of lake stages are marked by erosional and correlative surfaces, and are characterized by gamma ray marker peaks and long-term changes in Fischer assay logs i.e., oil shale richness (Fig. 7.3, Stage boundaries).

The evolution and progression of lake stages in the Piceance basin are consistent with the global Eocene climate trend. Additionally, lake stages also record a deepening-upward trend followed by a late siliciclastic fill that reflect larger-scale changes in the basin caused by tectonics and climate (Fig. 7.9; Table 7.2). Lake stages represent the main Green River Formation lake interval in the Piceance basin. However, the exact timing and the length of each lake stage is not well established because of incomplete age control. There are only three tuff beds that have been dated and correlated into the Piceance basin (after Smith et al. 2008, 2010) (Fig. 7.9). To estimate the chronology of the Green River Formation study interval and the position of lake stages, rich and lean zones, sequence boundaries, available age dates and stratigraphic studies done by Smith et al. (2008, 2010) and Davis et al. (2009) were used (see Fig. 7.9).

The initial Stage 1 (Fresh to mesosaline lake) marks the beginning of a large, single lake basin, formed before the Eocene climate optimum, and characterized by fresh to mesosaline (i.e., higher salinity, but below the level for precipitation of dawsonite, nahcolite, or gypsum) water conditions. This stage includes from the molluscan-rich Long Point Bed at the base of the Green River up through the organic-rich illite shale of the R1 zone (Figs. 7.3 and 7.9). The beginning of Stage 2 (Transitional lake) marks the beginning of important mineralogical and depositional changes in the lake and occurred during the beginning of the Eocene climate optimum. The deposition along the basin margin is characterized by relatively high siliciclastic input and formation of the first thick microbial carbonate deposits. Basinward, the clay-rich oil shale was replaced by the carbonate-rich oil shale and the first evaporite deposition occurred (dawsonite followed by nahcolite). Stage 2 encompasses the L1 through L3 interval of the Green River (Figs. 7.3 and 7.9). The R2 and R3 rich zones are on average less rich then the underlying fresh-lake R1 or the overlying R4 zone (see Fig. 7.3 and Feng 2011). Lake stages 1 and 2 fall under the balanced fill lake of Bohacs et al. (2000). Following Stage 3 (Highly fluctuating lake) represents an underfilled lake (Bohacs et al. 2000) and formed during the peak of the Eocene climate optimum. It is characterized by thick evaporite intervals and highly fluctuating cycles from shallow to deeper lake environments, indicating rapid fluctuation between dry and wet times during the hot house of the optimum. This stage includes from the R4 through the L5 zones (Figs. 7.3 and 7.9). Both the R4 and R5 can be very rich, although they are generally diluted by increased nahcolite precipitation within these intervals (Feng 2011). The following stage, Stage

Table 7.2 Overview and short descriptions of lake stages (S) in the Piceance basin

Lake stage	Description
S1	Beginning of stage marks lake-wide transgression and beginning of large lake system. Laterally continuous, progradational to aggradational depositional units dominate. Along the margins carbonate shoals (FA4) and channelized delta (FA5) deposits formed. In the deeper basin area Type 2 depositional units and clay-rich oil shale (FA10 and FA11) deposits formed. Deposits are rich in fish remains and ostracods, especially in the earlier part of the stage. Organic-rich deposits resulted in high runoff and high nutrient input (R0 and R1). The richest deposits formed in the upper part of the stage (R1)
S2	Beginning of stage marks rapid increase in siliciclastic input at the marginal areas, dominance of laterally discontinuous progradational to aggradational highly cyclic deposits, changes in mineralogy, and first appearance of thick microbial carbonates (FA6). Thick sandstone units (FAs3, 5, and 7) capped with thick carbonate shoals (FA4) and microbial carbonates (FA6) formed along the basin margins. In the deeper lake areas, clay-rich oil shales where replaced with carbonate-rich oil shales (FA10 and FA11) and evaporite (FA13) deposition increased upwards within stage. In the deepest part of the basin, Type 3 depositional units formed that changed to Type 2 depositional units towards margins. Richest organic-rich deposits formed as oil shale breccias (FA11.2) in the deepest portion of the lake. Richest deposits formed during the beginning of the stage (R2), whereas increased lake restriction and salinity lead to higher dilution of organics upwards (during R3)
S3	Deposition of aggradational to retrogradational highly cyclic, laterally discontinuous depositional units. Thick sandstone units (FAs3, 5, and 7) capped with thick microbial carbonates (FA6) formed along the basin margins. Clastic input and deposits into the marginal areas decreased upwards within stage. In the profundal area, Type 3 depositional units, with thick evaporite (FA13) deposits dominate. The richest oil shale deposits occur dominantly as discontinuous oil shale breccia (FA11.2) deposits that form very thick stacked depositional packages in the deeper part of the basin and thin towards the basin margins. Especially thick and very rich oil shale breccia deposits formed during the first part of the stage (R4). In the upper part, extensive evaporite deposition led to the higher dilution of organic material and to somewhat leaner deposits
S4	Lateral increase of profundal FAs (FAs10 to 12) and laterally continuous depositional units. Previous marginal deposits (FAs1 to 8) were covered by the profundal deposits (FAs10 to 12). Increase in fluvial input caused decrease in salinity and evaporites and increase in nutrient supply. Type 2 depositional units dominate in the profundal part
S5	High runoff resulted in high lake level. Profundal, laterally continuous FAs dominate (FAs10 to 12), with Type 2 depositional units occur over most of the deep basin area. Some evaporite deposition (early diagenetic nahcolite nodules, FA13.1) occurred in the southern and western parts of the basin. Rich oil shales formed as laminated oil shales (FA10) and as oil shale breccias (FA11.2)
S6	Progradation of siliciclastics from north to south, and closing of the basin. Evaporites, as nahcolite nodules and in places crystals (FA13.1), occur in deposits in the southern part of the basin. Laminated oil shale (FA10) and soft-sediment-deformed oil shale (FA11.1) deposits interfinger with Uinta Formation sandstones. Some rich oil shale occurs in the southern part of the lake

4 (Rising lake) includes the R6 rich zone and formed after the Eocene climate optimum. It is characterize by the increasingly deeper profundal oil shale deposits, indicating an overall increase in runoff and lake level rise (Figs. 7.3 and 7.9). Stage 5 (High lake) marks the time period of the high lake level, when profundal, rich oil shale deposits of the Mahogany zone (R7) can be correlated over much of the basin area (Figs. 7.3 and 7.9). Lake stages 4 and 5 would be classified as balanced fill lakes (Bohacs et al. 2000). Stage 6 (Closing lake) marks the beginning of the closing of the lake and is an overfilled lake (Bohacs et al. 2000). Siliciclastic deposits from the north prograded southwards and finally filled in the Piceance lake basin (Figs. 7.3 and 7.9). The final fill with

Fig. 7.9 (continued) hypothermals. Lake stages after Tänavsuu-Milkeviciene and Sarg (2012), age data and related correlation after Smith et al. (2008, 2010), rich and lean zones after Cashion and Donnell (1972, 1974), Mercier et al. (2009), Johnson et al. (2010), geomagnetic polarity timescale, Eocene boundaries, negative carbon isotope excursions, and hyperthermals after Zachos et al. (2001, 2008, 2010), Sexton et al. (2006, 2011), Dutton et al. (2005), Lourens et al. (2005), Nicolo et al. (2007), Bijl et al. (2009)

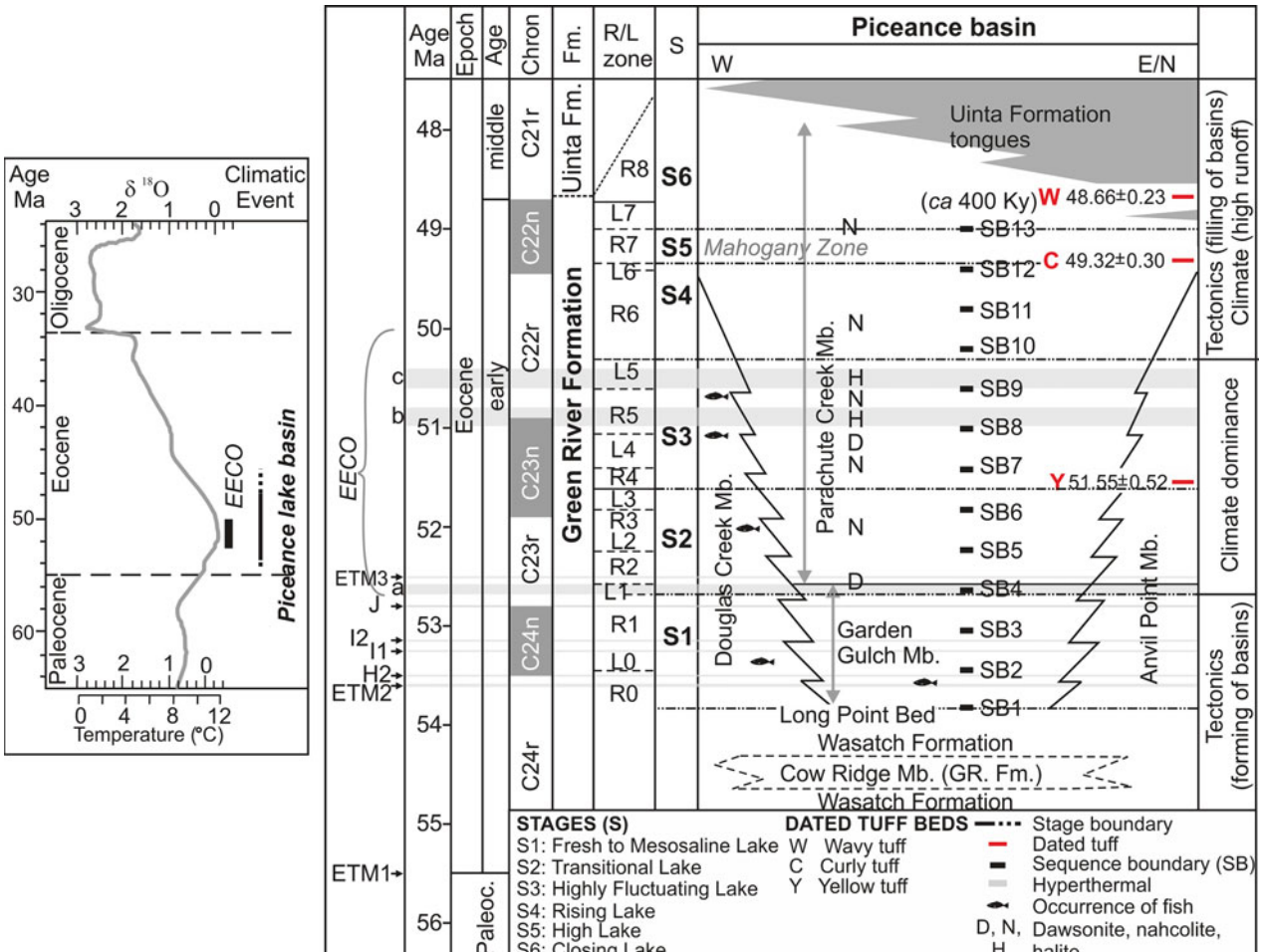

Fig. 7.9 Piceance basin stratigraphy and age model (After Smith et al. 2008, 2010) in correlation with Eocene climate curve and Early Eocene Climate Optimum (EECO) (After Zachos et al. 2001), and position of stages (*S*), rich (*R*) and lean (*L*) zones, and sequence boundaries (*SB*). Lake stages were separated based on the depositional trends of the facies associations in the Piceance basin. Position of rich and lean oil shale zones is based on the correlation between lake stages and rich and lean zones. Position of large-scale sequences (*ca* 400 Ky) is marked by major facies association changes, major changes in oil shale richness, gamma ray signals, Fischer assay logs, and

siliciclastics was probably the result of the combination of increased tectonic activity, weathering, erosion, and inflow (Carroll et al. 2006; Smith et al. 2008; Davis et al. 2009; Chetel et al. 2011; Tänavsuu-Milkeviciene and Sarg 2012).

7.5.2 Depositional Architecture

Based on vertical and lateral variation of facies associations three idealized depositional cycles have been recognized that characterize depositional pattern in the lake from littoral lake margin to deeper sublittoral and finally profundal environments (Fig. 7.10a).

Type 1 depositional cycles occur along basin margins and in the photic zone of the lake. Type 1 depositional cycles are bounded by erosional boundaries. These cycles starts either by erosionally based structureless alluvial (FA1) or delta (FA5) deposits or by littoral to sublittoral siliciclastic (FA7) deposits. In places, shoreline sandstones occur. Littoral to sublittoral undefined silicicilastic (FA7) deposits most probably present distal part of delta front. On log data, the beginning of depositional cycle is marked by gamma-ray peak that occurs just below the erosion-based sandstones (Fig. 7.3). Siliciclastic deposits that mark the lower boundary of sequences contain abundant load structures and dewatering structures that suggest rapid deposition. In vertical section siliciclastic deposits display overall upward-coarsening and upward-shallowing trends (Fig. 7.5b). This is supported by vertical changes from littoral and sublittoral siliciclastics (FA7) upwards into delta (FA5) or shoreline (FA3) deposits. Progradational siliciclastic deposits are overlain by sharp based carbonate deposits, composed of interbedded carbonate shoal (FA3) and microbial carbonate (FA6) deposits. Carbonate deposits change vertically from intraclastic breccia, intraclastic rudstone, coated grains, or with a mixture of different carbonate grains and clasts into microbial carbonates that pass from agglutinated, dendrolitic stromatolites and thrombolites to fine-grained laminated stromatolites indicating an overall upward-deepening trend (Sarg et al. 2013). Carbonate deposits are abruptly covered by clay- or carbonate-rich mudstones or siltstones (FA8). In places lean, sublittoral oil shale (FA9) formed in the upper part of these sequences (Fig. 7.10a).

In the profundal zone, cycle boundaries are conformable, and are marked by sharp changes in organic richness of deposits. Type 2 depositional cycle character occurs basinward from the Type 1 depositional cycle. Type 2 depositional cycle begin either with lean laminated oil shale (FAs 9, 10) or with sublittoral mudstones and siltstones (FA8). Thin layers and beds of silt and very fine-grained sandstones occur in these deposits. Lean oil shale (FAs 9, 10) deposits or sublittoral mudstone and siltstone (FA8) deposits are followed by meter to decimeter thick siliciclastic turbidite intervals (FA12). Turbidites (FA12) form normally graded or soft-sediment-deformed, sharp-based sandstone units interbedded with sublittoral mudstones and siltstones. Organically lean deposits are sharply overlain by organic rich laminated oil shale (FA10) and gravitational oil shale (FA11) deposits (Fig. 7.10a). Sharp boundaries between organic rich and organic lean deposits is well seen on Fischer assay logs (Fig. 7.3, L and R zones), and are marked by gamma ray peaks.

Deposits of Type 3 depositional cycle occur in the most basinward position from Type 1 and Type 2 depositional cycles. The beginning of Type 3 depositional cycles are marked by evaporite deposits, halite and nahcolite crystal accumulations and nodules or by lean oil shale deposits that contain large amounts of disseminated nahcolite crystals. No silt or sandstone beds have been found in Type 3 cycles. The lower portion of these depositional cycles is comprised of lean oil shale that is sharply overlain by organic-rich laminated oil shale (FA10) or gravitational oil shale (FA11) deposits (Fig. 7.10a). This turnaround in organic richness is similarly to Type 2 and is very well marked on Fischer assay logs (see also Fig. 7.3, L and R zones) and are represented as peaks on gamma ray logs (Fig. 7.3).

Depositional cycles vary greatly in thickness and in lateral extension and can be followed in outcrops. Type 1 depositional cycle vary laterally over relatively short distances, from meters to

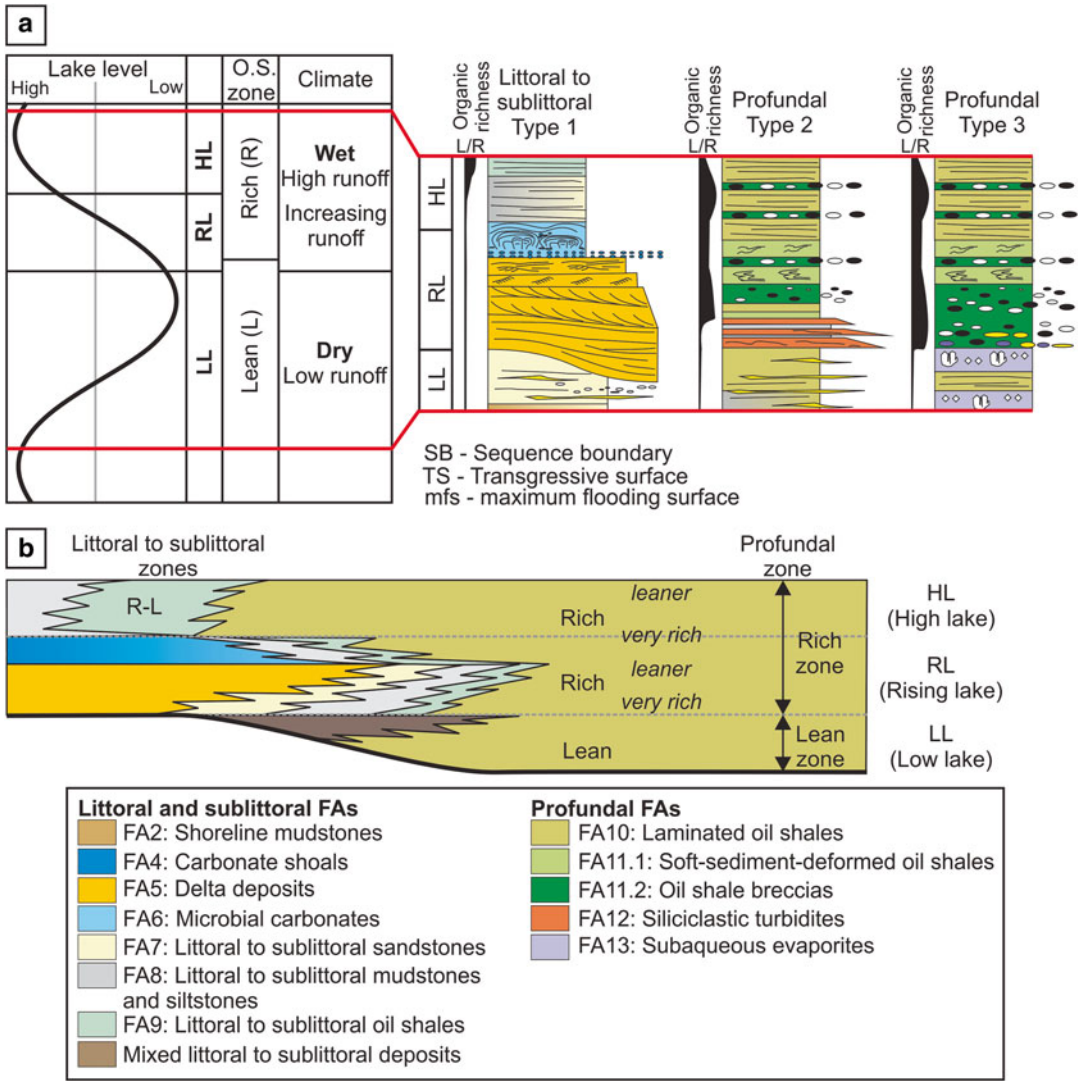

Fig. 7.10 Idealized depositional cycles and depositional sequences of the Piceance basin lake deposits. Based on this model deposition was dominantly controlled by the climate changes from dry to humid. (**a**) Three idealized depositional cycles for the littoral to sublittoral and profundal lake zones. (**b**) Composite depositional model for the large-scale depositional sequences in the lake system that shows the lateral and vertical variation of facies associations and distribution of organic-rich material across the basin (Modified from Tänavsuu-Milkeviciene et al. 2012)

hundreds of meters (Fig. 7.5a, e and 7.6c). Type 2 and Type 3 depositional cycles are usually more stable and can be followed over longer distances over hundreds of meters. However, single cycles vary too greatly to be followed in subsurface.

Stacked depositional cycles described above form depositional sequences, metres to 10s of metres thick correlative units that are bounded by surfaces that can be recognized regionally; are characterized by erosional surfaces, strong shifts in facies associations basinward, show rapid decline in oil shale richness, and prominent peaks on well logs (Fig. 7.3). Depositional sequences are at the scale of the well correlated rich and lean oil shale zones and large scale facies association shifts. Altogether, 13 depositional sequences have been recognized (see Fig. 7.3).

7.6 Discussion and Depositional Model

Deposition in the littoral to sublittoral zones is characterized by overall upward-fining cycles. However, single sandstone rich facies associations (FAs3, 5, 7) within the cycle form dominantly progradational, upward-coarsening deposits. Facies association changes within cycles are marked by sharp, in part erosional boundaries, from mudstones to sandstones, and from sandstones to carbonates suggesting abrupt changes in lake conditions. Mudstones and oil shale abruptly overlie carbonates due to drowning. In addition, regional metre-scale depositional sequences appear to be correlative across the lake basin, suggesting allocyclic control on the large scale stratigraphy.

Deposition in lacustrine settings is cyclic in nature and it is not controlled by global sea/level changes but by changes climate and tectonics. These may include changes in fresh water runoff from the catchment area and the intensity of evaporation. The tectonic regime of the area has direct impact on local climate, and changes in local lake basin morphology. Tectonically induced changes generally have timespans on the order of 100's of thousands to millions of years. They will affect the whole lake basin by either increasing or decreasing subsidence, changing provenance terrains, and/or changing catchment area relief. The Green River Formation fill of the Piceance basin suggests early moderate subsidence that resulted in thicker early Green River fill in Stage 1, subsequently slowed, than increased again in Stage 3, and then slowed during Stages 4 and 5 (see Fig. 7.3). Subsidence then increased again during the closing Stage 6. This periodicity occurred over 2 my time periods (Fig. 7.9)

Climate changes can occur on over a range of frequencies from very short on the scale of decadal wet and dry cycles to 100,000 year plus climatic changes related to global warm/cool temperature cycles (i.e., solar forcing Milankovitch cyclicity). Because lakes are closed systems, climate has very strong influence on deposition. Therefore, switches in regional climate system from more humid to more arid control variation in runoff and vegetation, as well as intensity of chemical and physical weathering and this in turn affects inflow of siliciclastics and nutrients into the lake. The depositional cycles identified in this study appear to be at a higher frequency than the tectonic changes suggested by accommodation cycles. Therefore, based on an understanding of climate influence on deposition in lakes, a climate based depositional model is proposed below to explain formation depositional sequences in the Piceance Lake. The periodicity of the 13 depositional sequences identified here is suggested to be on the 400 Kyr Milankovitch eccentricity cycles, based on correlation to the absolute age dates documented in the greater Green River system (Smith et al. 2008, 2010) (Fig. 7.9).

During times of low precipitation rates and dry climate period overall hydrologic input decreases (Fig. 7.10a). Main inflow into the lake was by groundwater inflow and/or flash-flood runoff (Sewall and Sloan 2006; Lyons et al. 2011). Sporadic and limited runoff and lower inflow led to lowering of lake level. Decreased precipitation also resulted in limited nutrient inflow into the lake and led to a decline in algal production. Deposition along lake margins was dominated by overbank and dryland river deposits (FA1) and marginal mudstones (FA2) (see example Fig. 7.5a–d). At times, strong, but intermittent flash-flood deposits could form. Low lake level deposits along the basin margins are not well preserved, however. This could be caused by the erosion and reworking of possibly relatively thin deposits during following rising lake. In places, low lake level deposits are preserved basinward. The thickest deposits preserved in the profundal zone as lean oil shale deposits, or lean oil shale deposits interbedded with nahcolite and halite beds (see example Fig. 7.8b, g, h) (Fig. 7.10).

During the change to a wetter period, increased precipitation and runoff resulted in stronger erosion and higher physical weathering of the surrounding areas. Higher inflow and as a consequence, increased sediment and nutrient input into the lake led to lake level rise. Along

basin margins lake level rise is well marked by erosionally-based channel or carbonate lag and shoal deposits (Figs. 7.5c and 7.10). Rip-up siliciclastic and carbonate clasts, mudstone clasts, tree branches, fish scales and fragments occur at erosional boundaries (Fig. 7.6e, f). Soft-sediment deformations are abundant on the base of siliciclastic deposits.

Increased runoff increased erosion of surrounding areas and was followed by transport of nutrients into the lake. Due to increased nutrient input algal and bacterial colonies bloomed and the beginning of the rising lake is marked by sharp increase in organic-richness of profundal lake deposits (Fig. 7.10) (Feng 2011). In places, in deeper sublittoral areas the beginning of the rising lake was also marked by sharply based siliciclastic turbidites (FA12) (Fig. 7.10a). Similar observations have been described by other studies (Harris et al. 2005; Lyons et al. 2011).

During the ensuing humid climate period, inflow into the lake remained high due to high river and groundwater inflow, resulting in high lake levels (Fig. 7.10a). Higher inflow into the lake resulted in the most widespread and deepest lake condition (Fig. 7.10). High nutrient input enhanced productivity and in cases of anoxic bottom conditions preservation potential of organic matter increased hugely. This resulted in formation of the most widespread rich oil shale deposits (Fig. 7.10).

The organic-rich and organic-lean mudrocks within the Piceance basin can be related in distribution to their position within depositional sequences. Low lake deposits form lean oil shale deposits that can be separated in the deeper part of the basin, but thin out towards the basin margins. Along the basin margins, thick siliciclastic and carbonate deposits formed during rising lake and are followed by littoral to sublittoral mudstones and oil shale deposits formed during high lake. These deposits are equivalent to the rich oil shale deposits formed during the rising and high lake in the deeper part of the basin. Richness decreases from the profundal areas to the basin margin within these mud rocks (see also Feng 2011).

7.7 Conclusions

The Piceance basin formed as a mixed carbonate-siliciclastic and evaporite-rich deep, stratified organic-rich lake basin in the early to middle Eocene age. Altogether, 24 facies and 13 facies association have been described from the basin area. Most of the deposits formed in the profundal zone as laminated oil shale, gravitational oil shale, siliciclastic turbidites, or subaqueous evaporites. Along the lake margin, alluvial and littoral to sublittoral deposits, shoreline mudstones, shoreline sandstones, carbonate shoals, microbial carbonates, delta, and littoral to sublittoral mudstones to sandstones, and oil shale deposits formed.

Long-term changes in lake are reflected by lake stages (tens to hundreds of meters). Lake stages are controlled by a combination of climate and tectonics that regulate variation in sedimentological patterns, depositional trends, and organic-richness throughout the basin evolution. Stage 1, Fresh to mesosaline lake, was deposited during decreasing tectonic activity and increasing climate control. Lake Stages 2 and 3, Transitional and Highly fluctuating lake periods are interpreted to have been dominated by an increasingly warm and arid climate during the Early Eocene Climate Optimum. Following Stages 4, 5, and 6, Rising, High, and Closing lake periods record the change to a wetter climate and increasing tectonic activity, resulting in a widespread deep lake and increased siliciclastic input that extended across the Piceance basin.

Three depositional cycles have been described, one from the littoral and sublittoral zone and two from the profundal zone, Type 1, Type 2 and Type 3 respectively. Depositional cycles combine into larger-scale depositional sequences that display similar depositional patterns. Altogether 13 depositional sequences (10s of metres thick) have been defined within the Green River Formation in the Piceance basin. They display significant changes in lake regime and are divided into periods of low, rising, and high lake that are separated by erosional surfaces, prominent facies association shifts, and drastic changes in richness of deposits.

A climate model is proposed for formation of the depositional sequences and is suggested to control the formation of organic rich and lean deposits. Facies within sequences and organic-rich mudrocks are controlled by variations in run-off and vegetation that influence the inflow of siliciclastics and nutrients, and the formation and distribution of organic-rich deposits. Organic richness of deposits varies vertically and laterally within depositional sequences. The richest deposits form dominantly in the beginning or latter part of the rich units in early rising and late high lake level times. During low lake, organic lean deposits formed in the deeper part of the basin and thin out towards the basin margins. The rising lake is marked by thick siliciclastic and carbonate deposits along the basin margin, and rich oil shale deposits in the deeper part of the basin. During the following high lake, littoral to sublittoral deposits formed along the basin margins, whereas in the profundal zone rich oil shale deposits were deposited.

Acknowledgments This work is part of the Colorado School of Mines COSTAR oil shale project, financed by ExxonMobil, Total and Shell. We thank the USGS Core Research Center in Denver for providing the core data. We also thank Martynas Milkevičius and Suriamin for help with fieldwork and photography.

References

Arnott RWC (2010) Deep-marine sediments and sedimentary systems. In: James NP, Dalrymple RW (eds) Facies models, vol 6, Geological Association of Canada IV Series. GEOtext, St. John's, pp 295–322

Bhattacharya JP, Giosan L (2003) Wave-influenced deltas: geomorphological implications for facies reconstruction. Sedimentology 50:187–201

Bijl PK, Schouten S, Sluijs A, Reichart G-J, Zachos JC, Brinkhuis H (2009) Early Palaeogene temperature evolution of the southwest Pacific Ocean. Nature 461:776–779

Boak J, Sheven P (2015) Mineralogy of the Green River Formation in the Piceance Creek Basin, Colorado. In: Smith ME, Carroll AR (eds) Limnogeology of the Eocene Green River Formation: synthesis in limnogeology. Springer, Dordrecht, pp 183–209

Bohacs KM, Carroll AR, Neal JE, Mankiewicz PJ (2000) Lake-basin type, source potential, and hydrocarbon character: an integrated sequence-stratigraphic-geochemical framework. In: Gierlowski-Kordesch EH, Kelts KR (eds) Lake basins through space and time, vol 46, AAPG studies in geology. American Association of Petroleum Geologists, Tulsa, pp 3–34

Bouma AH (1962) Sedimentology of some Flysch deposits. Elsevier, Amsterdam, 168 p

Bray TF Jr, Carter CH (1992) Physical processes and sedimentary record of a modern, transgressive, lacustrine barrier island. Mar Geol 105:155–168

Bridge JS, Demicco RV (2008) Earth surface processes, landforms and sediment deposits. Cambridge University Press, Cambridge, p 815

Brownfield ME, Mercier TJ, Johnson RC, Self JG (2010) Nahcolite resources in the Green River Formation, Piceance Basin, Colorado. U.S. Geological Survey, Reston Digital Data Series, DDS-69-Y, Chp. 2. 51 p

Buatois LA, Mangano MG (1995) Sedimentary dynamics and evolutionary history of a Late Carboniferous Gondwanic lake in north-western Argentina. Sedimentology 42:415–436

Carroll A, Chetel LM, Smith ME (2006) Feast to famine: sediment supply control on Laramide basin fill. Geology 34:197–200

Cashion WB, Donnell JR (1972) Chart showing correlation of selected key units in the organic-rich sequence of the Green River Formation, Piceance Creek Basin, Colorado, and Uinta Basin, Utah. U.S. Geological Survey, Reston Oil and Gas Investigations, Chart OC-65

Cashion WB, Donnell JR (1974) Revision of nomenclature of the upper part of the Green River Formation, Piceance Creek Basin, Colorado, and Eastern Uinta Basin, Utah. U.S. Geological Survey, Bulletin, 1394-G, 9 p

Chetel LM, Janecke SU, Carroll AR, Beard BL, Johnson CM, Singer BS (2011) Paleogeographic reconstruction of the Eocene Idaho River, North American Cordillera. Geol Soc Am Bull 123:71–88

Clementz MT, Sewall JO (2011) Latitudinal gradients in greenhouse seawater $\delta^{18}O$: evidence from Eocene sirenian tooth enamel. Science 332:455–458

Cohen AS (2003) Paleolimnology: the history and evolution of lake systems. Oxford University Press, Oxford, 528 p

Cohen AS, Talbot MR, Awramik SM, Dettman DL, Abell P (1997) Lake level and paleoenvironmental history of Lake Tanganyika, Africa, as inferred from late Holocene and modern stromatolites. Geol Soc Am Bull 109:444–460

Cole RD, Daub GJ (1991) Methane occurrences and potential resources in the lower Parachute Creek Member of Green River Formation, Piceance Creek Basin, Colorado. In: 24th Oil Shale symposium proceedings: Colorado School of Mines Quarterly, vol 83, Golden, pp 1–7

Davis SJ, Mulch A, Carroll AR, Horton TW, Chamberlain CP (2009) Paleogene landscape evolution of the

central North American Cordillera: developing topography and hydrology in the Laramide foreland. Geol Soc Am Bull 121:100–116

Demaison GJ, Moore GT (1980) Anoxic environments and oil source bed genesis. Am Assoc Pet Geol Bull 64:1179–1209

Dickinson WR, Klute MA, Hayes MJ, Janecke SU, Lundin ER, McKittrick MA, Livares MD (1988) Paleogeographic and paleotectonic setting of Laramide sedimentary basins in the central Rocky Mountain region. Geol Soc Am Bull 100:1023–1039

Dutton A, Lohmann KC, Leckie RM (2005) Insights from the Paleogene tropical Pacific: foraminiferal stable isotope and elemental results from Site 1209, Shatsky Rise. Paleoceanography 20:16p

Dyni JR (1981) Geology of the nahcolite deposits and associated oil shales of the Green River Formation in the Piceance Creek Basin, Colorado. PhD thesis, University of Colorado, Boulder, 144 p

Dyni JR (2006) Geology and resources of some world oil-shale deposits. U.S. Geological Survey, Reston Scientific Investigation Report, 2005–5294, 42 p

Dyni JR, Hawkins JE (1981) Lacustrine turbidites in the Green River Formation, northwestern Colorado. Geology 9:235–238

Feng J (2011) Source rock characterization of the Green River Oil Shale, Piceance Creek Basin, Colorado. MSc thesis, Colorado School of Mines, Golden, 84 p

Ghadeer SG, Macquaker JHS (2012) The role of event beds in the preservation of organic carbon in fine-grained sediments: analyses of the sedimentological processes operating during deposition of the Whitby Mudstone Formation (Toarcian, Lower Jurassic) preserved in northeast England. Mar Pet Geol 35:309–320

Gierlowski-Kordesch EH (2010) Lacustrine carbonates. In: Alonso-Zarza AM, Tanner LH (eds) Carbonates in continental settings: facies, environments, and processes, vol 61, Developments in sedimentology. Elsevier, Amsterdam/London, pp 1–101

Gierlowski-Kordesch EH, Rust BR (1994) The Jurassic East Berlin Formation, Hartford basin, Newark Supergroup (Connecticut and Massachusetts): a saline lake-playa-alluvial plain system. In: Renaut RW, Last WM (eds) Sedimentology and geochemistry of modern and ancient saline lakes, vol 50, SEPM Special Publications. SEPM, Tulsa, pp 249–265

Hardie LA, Smoot JP, Eugster HP (1978) Saline lakes and their deposits: a sedimentological approach. In: Matter A, Tucker ME (eds) Modern and ancient lake sediments, vol 2, International Association of Sedimentologists, Special Publication. Blackwell Scientific, Oxford, pp 1–6

Harris NB, Freeman KH, Pancost RD, Mitchell GD, White TS, Bate RH (2005) Patterns of organic-carbon enrichment in a lacustrine source rock in relation to paleo-lake level, Congo Basin, West Africa. In: Harris NB (ed) The deposition of organic-carbon-rich sediments: models, mechanisms, and consequences, vol 82, SEPM Special Publications. SEPM, Tulsa, pp 103–123

Ilgara A, Nemec W (2005) Early Miocene lacustrine deposits and sequence stratigraphy of the Ermenek Basin, Central Taurides, Turkey. Sediment Geol 173:233–275

Johnson RC (1984) New names for units in the lower part of the Green River Formation, Piceance Creek Basin, Colorado. U.S. Geological Survey, Bulletin, 1529-I, 20 p

Johnson RC (2012) The systematic geologic mapping program and a quadrangle-by-quadrangle analysis of time-stratigraphic relations within oil shale-bearing rocks of the Piceance Basin, western Colorado. U.S. Geological Survey, Scientific Investigations Report 2012–5041, 28 p

Johnson CL, Graham SA (2004) Cycles in perilacustrine facies of late Mesozoic rift basin, southeastern Mongolia. J Sediment Res 74:786–804

Johnson RC, Nichols DJ, Hanley JH (1988) Stratigraphic sections of Lower Tertiary strata and charts showing palynomorph and mollusk assemblages, Douglas Creek Arch area, Colorado and Utah, U.S. Geological Survey, Miscellaneous field studies map. The Survey, Reston

Johnson RC, Mercier TJ, Brownfield ME, Pantea MP, Self JG (2010) An assessment of in-place oil shale resources in the Green River Formation, Piceance Basin, Colorado. U.S. Geological Survey, Reston Digital Data Series DDS–69–Y, Chp. 1, 187 p

Keighley D (2008) A lacustrine shoreface succession in the Albert Formation, Moncton Basin, New Brunswick. Bull Can Petrol Geol 56:235–258

Kelts K (1988) Environments of deposition of lacustrine petroleum source rocks: an introduction. In: Fleet AJ, Kelts K, Talbot MR (eds) Lacustrine petroleum source rocks, vol 40, Geological society special publications. Published for the Geological Society by Blackwell Scientific Publications, Oxford/Boston/Edinburgh/Palo Alto/Melbourne, pp 3–26

LaClair D, Lowenstein TK (2009) Fluid inclusion microthermometry from halite in the Eocene Green River Formation, Piceance Creek basin, Colorado, USA: evidence for a perennial stratified saline lake. Geological Society of America, annual meeting, abstracts with programs, Portland, 41, p 512

Last WM, Vance RE (1997) Bedding characteristics of Holocene sediments from salt lakes of northern Great Plains, Western Canada. J Paleolimnol 17:297–318

Lourens LJ, Sluijs A, Kroon D, Zachos JC, Thomas E, Röhl U, Bowles J, Raffi I (2005) Astronomical pacing of late Palaeocene to early Eocene global warming events. Nature 435:1083–1087

Lyons RP, Scholz CA, Buoniconti MR, Martin MR (2011) Late Quaternary stratigraphic analysis of the Lake Malawi Rift, East Africa: an integration of drill-core and seismic-reflection data. Palaeogeogr Palaeoclimatol Palaeoecol 303:20–37

McGlue MM, Soreghan MJ, Michel E, Todd JA, Cohen AS, Mischler J, O'Connell CS, Castañeda OS, Hartwell

RJ, Lezzar KE, Nkotagu HH (2010) Environmental controls on shell-rich facies in tropical lacustrine rifts: a view from Lake Tanganyika's littoral. Palaios 25:426–438

Mercier TJ, Brownfield ME, Johnson RC, Self JG (2009) Fischer assays of oil shale drill cores and rotary cuttings from the Piceance Basin, Colorado–2009 Update. U.S. Geological Survey, Reston Open-File Report 98–483, Version 2.0, 16 p

Milroy PG, Wright VP (2002) Fabrics, facies control and diagenesis of lacustrine ooids and associated grains from the Upper Triassic, southwest England. Geol J 37:35–53

Müller R, Nystuen JP, Wright VP (2004) Pedogenic mud aggregates and paleosol development in ancient dryland river systems; criteria for interpreting alluvial mudrock origin and floodplain dynamics. J Sediment Res 74:537–551

Nicolo MJ, Dickens GR, Hollis CJ, Zachos JC (2007) Multiple early Eocene hyperthermals: their sedimentary expression on the New Zealand continental margin and in the deep sea. Geology 35:699–702

Olariu C, Bhattacharya JP (2006) Terminal distributary channels and delta front architecture of river-dominated delta systems. J Sediment Res 76:212–233

Osleger DA, Heyvaert AC, Stoner JS, Verosub KL (2009) Lacustrine turbidites as indicators of Holocene storminess and climate: Lake Tahoe, California and Nevada. J Paleolimnol 42:103–122

Pitman JK (1996) Origin of primary and diagenetic carbonates in the lacustrine Green River Formation (Eocene), Colorado and Utah. U.S. Geological Survey, Bulletin, 2157, 17 p

Pitman JK, Johnson RC (1978) Isopach, structure contour, and resource maps of the Mahogany oil-shale zone, Green River Formation, Piceance Creek Basin, Colorado. U.S. Geological Survey Miscellaneous Field Investigations Map MF-958, scale 1:126,720. The Survey, Reston

Pitman JK, Pierce FW, Grundy WD (1989) Thickness, oil-yield, and kriged resource estimates for the Eocene Green River Formation, Piceance Creek Basin, Colorado. U.S. Geological Survey Oil and Gas Investigations Chart OC-132. The Survey, Reston

Platt NH, Wright VP (1991) Lacustrine carbonate facies models, facies distributions and hydrocarbon aspects. In: Anadon P, Cabrera L, Kelts K (eds) Lacustrine facies analysis, international association of sedimentologists, vol 13, Special publication. Blackwell Scientific Publications, Oxford, pp 57–74

Plummer PS, Gostin VA (1981) Shrinkage cracks; desiccation or synaeresis? J Sediment Petrol 51:1147–1156

Rainey DK, Jones B (2009) Abiotic versus biotic controls on the development of the Fairmont Hot Springs carbonate deposit, British Columbia, Canada. Sedimentology 56:1832–1857

Reading HG, Collinson JD (1996) Clastic coasts. In: Reading HG (ed) Sedimentary environments: processes, facies and stratigraphy, 3rd edn. Blackwell Science, Oxford, pp 154–231

Renaut RW, Gierlowski-Kordesch EH (2010) Lakes. In: James NP, Dalrymple RW (eds) Facies models, vol 6, Geological Association of Canada IV Series. GEOtext. St. John's, pp 541–575

Renaut RW, Owen RB (1991) Shore-zone sedimentation and facies in a closed rift lake: the Holocene beach deposits of Lake Bogoria, Kenya. In: Anadón P, Cabrera L, Kelts K (eds) Lacustrine facies analysis, vol 13, Special Publication, International Association of Sedimentologists. Blackwell Scientific, Oxford, pp 175–195

Renaut RW, Tiercelin J-J (1994) Lake Bogoria, Kenya rift valley – a sedimentological overview. In: Renaut RW, Last WM (eds) Sedimentology and geochemistry of modern and ancient saline lakes, vol 50, SEPM Special Publications. SEPM, Tulsa, pp 101–123

Sabato MM (2007) Recognition of trigger mechanisms for soft-sediment deformation in the Pleistocene lacustrine deposits of the Sant'Arcangelo Basin (Southern Italy): Seismic shock vs. Overloading. Sediment Geol 196:31–45

Sarg JF, Suriamin, Tänavsuu-Milkeviciene K, Humphrey JD (2013) Lithofacies, stable isotopic composition, and stratigraphic evolution of microbial and associated carbonates, Green River Formation (Eocene), Piceance basin. Am Assoc Pet Geol Bull 97:1937–1966

Schieber J (2011) Reverse engineering mother nature – Shale sedimentology from an experimental perspective. Sediment Geol 238:1–22

Scholz CA, Talbot MR, Brown ET, Lyons RP (2011) Lithostratigraphy, physical properties and organic matter variability in Lake Malawi Drillcore sediments over past 145,000 years. Palaeogeogr Palaeoclimatol Palaeoecol 303:38–50

Schomacker ER, Kjemperud AV, Nystuen JP, Jahren JS (2010) Recognition and significance of sharp-based mouth-bar deposits in the Eocene Green River Formation, Uinta Basin, Utah. Sedimentology 57:1069–1087

Schubel KA, Lowenstein TK (1997) Criteria for the recognition of shallow-perennial-saline-lake halites based on recent sediments from the Qaidam Basin, Wester China. J Sediment Res 67:74–87

Self JG, Brownfield ME, Johnson RC, Mercier TJ (2010a) Fischer assay histograms of oil shale drill cores and cuttings from the Piceance Basin, northwestern Colorado. U.S. Geological Survey, Reston Digital Data Series DDS–69–Y, chp. 7, 9 p

Self JG, Johnson RC, Brownfield ME, Mercier TJ (2010b) Stratigraphic cross sections of the Eocene Green River Formation in the Piceance Basin, Northwestern Colorado. U.S. Geological Survey, Reston Digital Data Series DDS–69–Y, chp. 5, 7 p

Sewall JO, Sloan LC (2006) Come a little bit closer: a high-resolution climate study of the early Paleogene Laramide foreland. Geology 34:81–84

Sexton PF, Wilson PA, Norris RD (2006) Testing the Cenozoic multisite composite $\delta^{18}O$ and $\delta^{13}C$ curves: new monospecific Eocene records from a single locality, Demerara Rise (Ocean Drilling Program Leg 207). Paleoceanography 21(PA2019):1–17

Sexton PF, Norris RD, Wilson PA, Pälike H, Westerhold T, Röhl U, Bolton CT, Gibbs S (2011) Eocene global warming events driven by ventilation of oceanic dissolved organic carbon. Nature 471:349–352

Shanmugam G (2000) 50 years of the turbidite paradigm (1950s-1990s): deep-water processes and facies models-a critical perspective: Marine. Pet Geol 17:285–342

Smith JW, Milton C (1966) Dawsonite in the Green River Formation of Colorado. Econ Geol 61:1029–1042

Smith DG, Jol HM, Smith ND, Kostaschuk RA, Pearce CM (2005) The wave-dominated Willial River Delta, Lake Athabasca, Canada: its morphology, radar stratigraphy, and history. In: Giosa L, Bhattacharya JP (eds) River deltas-concepts, models, and examples, vol 83, SEPM Special Publication. SEPM, Tulsa, pp 101–123

Smith ME, Carroll AR, Singer BS (2008) Synoptic reconstruction of a major ancient lake system: Eocene Green River Formation, western United States. Geol Soc Am Bull 120:54–84

Smith ME, Chamberlain KR, Singer BS, Carroll AR (2010) Eocene clocks agree: Coeval 40Ar/39Ar, U-Pb, and astronomical ages from the Green River Formation. Geology 38:527–530

Surdam RC, Stanley KO (1980) Effects of changes in drainage-basin boundaries on sedimentation in Eocene Lakes Gosiute and Uinta of Wyoming, Utah, and Colorado. Geology 8:135–139

Tänavsuu-Milkeviciene K, Sarg JF (2012) Evolution of an organic-rich lake basin – stratigraphy, climate, and tectonics: Piceance Creek basin, Eocene Green River Formation. Sedimentology 59:1735–1768

Tänavsuu-Milkeviciene K, Sarg JF, Bartov Y (2012) Climate control on sequence stratigraphy in organic-rich lake basin: green river formation, Greater Lake Uinta, Colorado and Utah. AAPG RMS, Grand Junction

Tanner PWG (1998) Interstratal dewatering origin for polygonal patterns of sand-filled cracks: a case study from late Proterozoic metasediments of Islay, Scotland. Sedimentology 45:71–89

Wakelin-King GA, Webb JA (2007) Upper-flow-regime mud floodplains, lower-flow-regime sand channels: sediment transport and deposition in a drylands mud-aggregate river. J Sediment Res 77:702–712

Wright VP (2012) Lacustrine carbonates in rift settings: the interaction of volcanic and microbial processes on carbonate deposition. In: Garland J, Neilson JE, Laubach SE, Whidden KJ (eds) Advances in carbonate exploration and reservoir analysis, vol 370, Special Publications. Geological Society, London

Wright VP, Marriott SB (2007) The dangers of taking mud for granted: lessons from Lower Old Red Sandstone dryland river systems of South Wales. Sediment Geol 195:91–100

Young RG (1995) Stratigraphy of green River Formation in Piceance Creek Basin, Colorado. In: Averett WR (ed) The Green River Formation in Piceance Creek and Eastern Uinta basins. Grand Junction Geological Society, Grand Junction, pp 1–13

Zachos JC, Pagani M, Sloan L, Thomas E, Billups K (2001) Trends, rhythms, and aberrations in global climate 65 Ma to present. Science 292:686–693

Zachos JC, Dickens GR, Zeebe RE (2008) An early Cenozoic perspective on green house warming and carbon-cycle dynamics. Nature 451:279–283

Zachos JP, McCarren H, Murphy B, Röhl U, Westerhold T (2010) Tempo and scale of late Paleocene and early Eocene carbon isotope cycles: implications for the origin of hyperthermals. Earth Planet Sci Lett 299:242–249